

This is an electronic reprint of the original article.

This reprint *may differ* from the original in pagination and typographic detail.

Author(s): Magdalena Pacwa-Płociniczak, Agata Kumor, Marta Bukowczan, Aki Sinkkonen, Marja Roslund, Tomasz Płociniczak

Title: The potential of enhanced phytoremediation to clean up multi-contaminated soil – insights from metatranscriptomics

Year: 2024

Version: Final draft

Copyright: The Authors 2024

Rights: CC BY-NC-ND 4.0

Rights url: <http://creativecommons.org/licenses/by-nc-nd/4.0/>

Please cite the original version:

Magdalena Pacwa-Płociniczak, Agata Kumor, Marta Bukowczan, Aki Sinkkonen, Marja Roslund, Tomasz Płociniczak,

The potential of enhanced phytoremediation to clean up multi-contaminated soil – insights from metatranscriptomics, *Microbiological Research*, Volume 284, 2024, 127738, ISSN 0944-5013,

<https://doi.org/10.1016/j.micres.2024.127738>.

All material supplied via *Jukuri* is protected by copyright and other intellectual property rights. Duplication or sale, in electronic or print form, of any part of the repository collections is prohibited. Making electronic or print copies of the material is permitted only for your own personal use or for educational purposes. For other purposes, this article may be used in accordance with the publisher's terms. There may be differences between this version and the publisher's version. You are advised to cite the publisher's version.

1 *The potential of enhanced phytoremediation to clean up multi-contaminated soil – insights from*
2 *metatranscriptomics*

3

4 Magdalena Pacwa-Płociniczak^{1*}, Agata Kumor¹, Marta Bukowczan¹, Aki Sinkkonen², Marja
5 Roslund², Tomasz Płociniczak^{1*}

6

7 ¹Institute of Biology, Biotechnology and Environmental Protection, Faculty of Natural
8 Sciences, University of Silesia in Katowice, Jagiellońska 28, 40-032 Katowice, Poland

9 ² Horticulture Technologies, Natural Resources Institute Finland, Itäinen Pitkätatu 4A, Turku,
10 Finland

11

12 Magdalena Pacwa-Płociniczak: magdalena.pacwa-plociniczak@us.edu.pl;

13 Agata Kumor: agata.kumor@us.edu.pl;

14 Marta Bukowczan: marta.bukowczan@us.edu.pl;

15 Aki Sinkkonen: aki.sinkkonen@luke.fi;

16 Marja Roslund: marja.roslund@luke.fi;

17 Tomasz Płociniczak: tomasz.plociniczak@us.edu.pl

18

19 * - corresponding authors: magdalena.pacwa-plociniczak@us.edu.pl;

20 tomasz.plociniczak@us.edu.pl; tel +48322009442

21

22 *Abstract*

23 This study aimed to (i) investigate the potential for enhanced phytoremediation to
24 remove contaminants from soil historically co-contaminated with petroleum hydrocarbons
25 (PHs) and heavy metals (HMs) and (ii) analyze the expression of crucial bacterial genes and

26 whole metatranscriptomics profiles for better understanding of soil processes during applied
27 treatment.

28 Phytoremediation was performed using *Zea mays* and supported by the *Pseudomonas*
29 *qingdaonensis* ZCR6 strain and a natural biofertilizer: meat and bone meal (MBM). In previous
30 investigations, mechanisms supporting plant growth and PH degradation were described in the
31 ZCR6 strain. Here, ZCR6 survived in the soil throughout the experiment, but the efficacy of
32 PH removal from all soils fertilized with MBM reached 32% regardless of the bacterial
33 inoculation. All experimental groups contained 2% (w/w) MBM. The toxic effect of this
34 amendment on plants was detected 30 days after germination, irrespective of ZCR6 inoculation.
35 Among the 17 genes tested using the qPCR method, only expression of the *acdS* gene, encoding
36 1-aminocyclopropane-1-carboxylic acid deaminase, and the CYP153 gene, encoding
37 cytochrome P450-type alkane hydroxylase, was detected in soils. Metatranscriptomic analysis
38 of soils indicated increased expression of methane particulated ammonia monooxygenase
39 subunit A (*pmoA-amoA*) by *Nitrosomonadales* bacteria in all soils enriched with MBM
40 compared to the non-fertilized control. We suggest that the addition of 2% (w/w) MBM caused
41 the toxic effect on plants via the rapid release of ammonia, and this led to high *pmoA-amoA*
42 expression. In parallel, due to its wide substrate specificity, enhanced bacterial hydrocarbon
43 removal in MBM-treated soils was observed. The metatranscriptomic results indicate that
44 MBM application should be considered to improve bioremediation of soils polluted with PHs
45 rather than phytoremediation. However, lower concentrations of MBM could be considered for
46 phytoremediation enhancement. From a broader perspective, these results indicated the superior
47 capability of metatranscriptomics to investigate the microbial mechanisms driving various
48 bioremediation techniques.

49

50 Keywords: phytoremediation; co-contamination; PGPR; *Pseudomonas qingdaonensis*; meat
51 and bone meal, metatranscriptomics

52

53 *1. Introduction*

54

55 The remediation of soil contaminated with a mixture of organic and inorganic pollutants
56 is an unsolved global problem (Chirakkara et al., 2016). Typically, such soils are excavated and
57 sealed *ex situ*, or treated chemically or electrokinetically (Chaukura et al., 2022; Sánchez-Castro
58 et al., 2023). Both techniques obviously destroy soil microbial ecosystems and usually also the
59 soil's physical structure. In turn, phytoremediation is considered as a promising, cost-effective
60 *in situ* method that restores the site while maintaining the physical structure and fertility of the
61 soil (Jia et al., 2023). In the case of co-contaminated areas, it is therefore necessary to use
62 solutions based on phytoremediation or its modification. Among modifications, biostimulation
63 via nutrients and/or oxygen supply or bioaugmentation of plant growth-promoting bacteria
64 (PGPB) with additional beneficial features, e.g., PH degradation and HM tolerance, could be
65 applied.

66 PGPB are beneficial soil microbes that upgrade plant production, increasing crop yield,
67 being a component of an integrated plant nutrient management system (Vandana et al., 2021).
68 They act via activation of mechanisms involving the production of phytohormones,
69 siderophores, and enzymes. Bacterial PGP mechanisms also involve nitrogen fixation, the
70 solubilization of phosphorus, and the production of antibiotics that protect plants from
71 pathogens (Glick, 1995). They may also reduce abiotic stresses in plants caused by pollutants
72 and can increase the tolerance towards them. Moreover, some auxin-producing plant growth-
73 promoting rhizobacteria (PGPR) can colonize the roots of plants and modify their architecture,
74 which mostly leads to enhanced lateral root branching and the development of root hairs

75 (Vacheron et al., 2013). This creates more extended niches that can be inhabited by PH-
76 degrading rhizobacteria, thus enhancing the rhizodegradation process. PGPR can also enhance
77 metal bioavailability and increase the metal translocation from roots to shoots of plants
78 (Płociniczak et al., 2019). The amendment of polluted soil with beneficial bacteria and/or
79 specific fertilizers can improve the total plant biomass and the range of the root system and thus
80 enhance the activity of rhizospheric and endophytic microorganisms involved in the
81 phytoremediation process (Marchand et al., 2018; Shtangeeva et al., 2004).

82 To overcome the difficulties in biological remediation of soils co-contaminated with
83 petroleum hydrocarbons (PHs) and heavy metals (HMs), we aimed to investigate a new,
84 multiway approach which will assess the exact potential of biostimulation and bioaugmentation
85 to increase the efficiency of this phytoremediation. We decided to use phytoremediation
86 because it is the only biological technique that allows for permanent removal of heavy metals
87 from the soil (Ullah et al., 2023). Additionally, the root system of plants creates an appropriate
88 niche for the degradation of organic pollutants by autochthonous microorganisms and/or strains
89 introduced by bioaugmentation (rhizodegradation) (Li et al., 2022). Since the preparation of a
90 bacterial inoculum on a large field scale is a time-consuming and expensive process, we also
91 decided to verify the validity of bioaugmentation by using biostimulation with meat and bone
92 meal (MBM) as a biofertilizer. In our experiments, *Zea mays*, HM-resistant and PH-degrading
93 *Pseudomonas qingdaonensis* ZCR6 strain, a representative of PGPR, and natural biofertilizer
94 (MBM) were applied to soil that had been historically contaminated with PHs and HMs (Zn,
95 Cd, and Cu). Since our main aim was to identify the key mechanisms determining the
96 effectiveness of phytoremediation of co-contaminated areas, we focused our research on
97 determining the impact of the applied treatments on the activity of soil microorganisms, which,
98 despite many studies on phytoremediation, has not been studied in detail so far. The modern
99 molecular techniques we used in our research allow the detailed monitoring of microbial

100 activity in soil, but they have not been used extensively in phytoremediation studies before.
101 Moreover, there are no reports on the use of metatranscriptomics to explain the impact of
102 applied treatments on the activity of soil microorganisms, which are the main factors degrading
103 PHs and also influencing plant growth, and therefore also the removal of HMs from the soil.

104 Thus to confirm or exclude the activity of ZCR6 after its introduction into soil, we
105 performed qPCR analysis to monitor the expression of chosen genes detected previously in the
106 genome of the ZCR6 strain, with the potential to enhance the bio- and phyto-remediation
107 processes. What is new in the context of phytoremediation research is the use of global analysis
108 of bacterial gene expression in soil during the bioremediation process.

109 This method can shed light on the relative importance of mechanisms that could support plant
110 growth or stimulate indigenous microorganisms in experimental groups treated only with
111 MBM, making bioaugmentation unnecessary and phytoremediation more economical. For this
112 reason, applying the metatranscriptomics approach, allowing the global analysis of gene
113 expression in the studied environment and taxonomical analysis, is recommended (Han et al.,
114 2022). Only this approach – rather than cultivation methods and other non-cultivation
115 biochemical methods such as phospholipid fatty acid (PLFA) analysis and community-level
116 physiological profiles (CLPP) – will allow us to determine which processes are crucial for the
117 effective cleaning of contaminated areas and which groups of bacteria are responsible for
118 carrying it out. Designing our experimental groups we hypothesized that the phytoremediation
119 system supported simultaneously with the ZCR6 strain and MBM would show higher efficiency
120 in pollutant removal compared to the control groups separately treated with ZCR6 or MBM.
121 We also assumed that after introduction into the soil, the ZCR6 strain would be able to express
122 the beneficial features and thus support the phytoremediation process. We also hypothesized
123 that the stimulation of autochthonous microorganisms by the addition of MBM may contribute
124 to increasing the effectiveness of phytoremediation to a similar or even greater extent than

125 bioaugmentation of the ZCR6 strain. Moreover, we expected that the metatranscriptomics
126 approach would reveal crucial pathways activated in soil under the applied biostimulation and
127 bioaugmentation treatments.

128

129 *2. Materials and methods*

130

131 *2.1 Soil*

132 Soil co-contaminated with hydrocarbons and heavy metals was collected from an industrial area
133 located in the vicinity of the Jadwiga Coke Plant in Zabrze (Upper Silesia, southern Poland,
134 50.336010, 18.826797). Loamy sand soil samples were collected from a depth of 0.2 m. Before
135 the experiment, the soil was passed through a 2 mm sieve and stored at 4 °C. According to the
136 FAO system, the soil was classified as Albic Luvisol (FAO, 2015). Its detailed chemical and
137 physical parameters are listed in Table S1.

138

139 *2.2 Bacterial strain*

140 The *Pseudomonas qingdaonensis* ZCR6 strain was isolated from the rhizosphere of *Zea mays*
141 growing in the soil used in this study. In laboratory conditions, the strain showed the activity of
142 several mechanisms potentially involved in plant growth promotion. The ZCR6 was able to
143 produce indole acetic acid (IAA), siderophores, and ammonia, solubilized $\text{Ca}_3(\text{PO}_4)_2$, and
144 showed activity of cellulase and 1-aminocyclopropane-1-carboxylic acid deaminase (ACCD)
145 at a high level. Apart from PGP activity, it showed surface-active properties, degradation
146 abilities against petroleum hydrocarbons, and resistance to Cd, Zn, and Cu. The detailed genetic
147 and biochemical characteristics of ZCR6 were described by Chlebek et al. (2022).

148

149 *2.3 Selection of a rifampicin-resistant mutant of the ZCR6 strain and fluorescent labeling*

150 A spontaneous rifampicin-resistant mutant was screened to monitor the fate of the ZCR6 strain
151 after its introduction into the co-contaminated soil. Because resistance to this antibiotic is not
152 common for soil bacteria (no rifampicin-resistant bacteria in the tested soil were detected), it is
153 a good marker of the presence of the inoculated strain in the soil and/or plant tissues. For this
154 purpose, the ZCR6 strain was plated on 0.1 Luria Bertani (LB) medium enriched with 10 μg
155 mL^{-1} rifampicin, 1% (v/v) crude oil and 3 mM ZnSO_4 . The grown colonies were reinoculated
156 on 0.1 LB plates with a progressively higher content of antibiotic (up to 150 $\mu\text{g mL}^{-1}$). The
157 stability of rifampicin resistance was confirmed by subculturing resistant ZCR6^{rf} on 0.1 LB
158 plates supplemented with crude oil and Zn, without the addition of rifampicin. The ZCR6^{rf}
159 strain had the same biochemical features as the parental ZCR6. The ZCR6^{rf} was then labeled
160 with enhanced green fluorescent protein (EGFP).

161 To label the rifampicin-resistant ZCR6 strain with EGFP, electrocompetent cells were prepared
162 according to Nigris et al. (2018) and transformed with the pMP4655 plasmid vector with
163 constitutive expression of the *egfp* gene (Bloemberg et al., 2000). Electrotransformation was
164 performed according to the protocol of Prieto and Mercado-Blanco (2008). The labeled cells of
165 the ZCR6^{rf+egfp} harboring plasmids were examined using a Nikon ECLIPSE-Ni-U stereo
166 microscope equipped with epifluorescence detection, 480/40 nm excitation and a 510 nm long
167 pass emission filter (Chlebek et al., 2020).

168

169 *2.4 Inoculum preparation*

170 Bacteria used for the inoculum preparation were cultured on 0.1 LB broth supplemented with
171 rifampicin (150 $\mu\text{g mL}^{-1}$), tetracycline (50 $\mu\text{g mL}^{-1}$), added to maintain the marker resistance
172 and pMP4655 plasmid expression, and crude oil at a concentration of 1% (v/v) in an orbital
173 shaker at 120 rpm (28 °C, 48 h). The number of bacteria in the inoculum was established based
174 on the optical density measurement and plating method. The appropriate volume of the bacterial

175 suspensions was centrifuged (5,000 rcf, 4 °C, 40 min, Sigma 4–16 K), and the bacterial pellet
176 was washed twice with sterile water and resuspended in sterile water. Thermally inactivated
177 bacteria were prepared similarly, and their suspension was then treated at high temperature by
178 autoclaving (121 °C, 1 atm, 30 min). The efficiency of the sterilization process was determined
179 using the plating method, and no bacterial growth was observed.

180

181 *2.5 Experimental setup*

182 The phytoremediation experiment was conducted under laboratory conditions using soil co-
183 contaminated with petroleum hydrocarbons and heavy metals, as described in Section 2.1. The
184 experiment included 4 treatments carried out in triplicate: (1) planted soil treated with meat
185 bone meal (MBM) and inoculated with the live ZCR6^{rf+egfp} strain (BL+MBM), (2) planted soil
186 treated with MBM and the thermally inactivated ZCR6^{rf+egfp} strain (BTI+MBM), (3) planted
187 soil treated with MBM and water (W+MBM), and (4) planted soil treated with water (W). In
188 the experiment, 72 separate pots were prepared (4 treatments × 3 replicates × 6 time points).

189 Before the experiment, the soil was air-dried and passed through a 2 mm sieve. Then, the soil
190 moisture was adjusted and maintained at 50% of the maximum water-holding capacity during
191 the entire experimental period. The pots (2 L volume, 20 cm height, 12 cm width, 12 cm length)
192 were filled with 1 kg (dry weight, DW) of polluted soil. In the case of MBM-containing
193 experimental groups, polluted soil was supplemented with this biofertilizer (2%, w/w, provided
194 by Honkajoki Oy, Honkajoki, Finland). Since the ZCR6 strain was isolated from the
195 rhizosphere of maize, *Z. mays* was chosen as the tested plant species to reduce the adverse
196 effects of inoculum incompatibility with the host plant. Additionally, *Zea mays* is a fast-
197 growing, high-biomass-producing species with tolerance to multiple HMs and phytoextraction
198 ability. It develops an extensive fibrous root system and, thus, a large zone of rhizosphere soil,
199 which is highly desirable for the effective rhizodegradation of hydrocarbons by soil

200 microorganisms (Agnello et al., 2016; Cao et al., 2022). Seeds of *Zea mays* (P9363, Corteva
201 Agriscience) were placed into the soil (2 per pot) and then covered with a 1-cm layer of soil.
202 The experiment was conducted in a growth room under controlled light (14-h photoperiod at
203 15,000 lux; temperature 23/18 °C; light/dark). After 2 weeks, the following treatments were
204 applied: i) 50 mL of the bacterial solution of the ZCR6 strain (10^8 cfu g⁻¹ DW of soil)
205 (BL+MBM), ii) 50 mL of thermally inactivated bacterial solution of the ZCR6 strain (10^8 cfu
206 g⁻¹ DW of soil used for preparation) (BTI + MBM), or iii) 50 mL of sterile water was added to
207 the soil (W+MBM and W). After plant treatment the experiment was conducted for 40 days.
208 Soil samples collected on days 3, 10, 20, 30, and 40 were immediately acquired for estimating
209 the ZCR6 strain number. All the soil samples were then stored at -80 °C prior to use. For
210 molecular and biochemical analyses, soil samples taken on days 20 and 40 were used.

211

212 *2.6 Number of ZCR6 cells in the soil*

213 The number of living cells of the ZCR6 strain in the soil was determined on days 1, 3, 10, 20,
214 30 and 40 after soil inoculation using the dilution-plate method. For this purpose, LB agar plates
215 supplemented with rifampicin (100 µg mL⁻¹) were used according to Pacwa-Płociniczak et al.
216 (2019).

217 Additionally, the number of ZCR6 cells was verified using flow cytometry. One gram of soil
218 was mixed with 9 mL of detergent solution (250 mM tetrasodium pyrophosphate [TSP; pH 8.0]
219 containing Tween 80 [0.5% final concentration]). The mixture was shaken for 20 min in a
220 vortex at room temperature. Then, 1 mL of Nycodenz solution (80% [w/vol] prepared in 50
221 mM TSP buffer) was added to a 15 mL Falcon tube, and after soil sedimentation for 1-2
222 minutes, 2 mL of soil slurry was added to the Falcon tube with Nycodenz solution. The mixture
223 was centrifuged at 4,650 rcf for 30 min. The supernatant containing bacterial cells was
224 transferred to new Falcon tubes and analyzed by flow cytometry (CyFlow SPACE).

225

226 *2.7 Determination of TPH concentration*

227 The total petroleum hydrocarbon concentration in the soil was determined for each pot before,
228 during, and after the bioremediation study and expressed as the concentration of hydrocarbons
229 with a carbon number between 10 and 40 (TPH_{C10-C40}) following ISO 16703:2011 according to
230 Pacwa-Płociniczak et al. (2016a).

231

232 *2.8 Heavy metal concentrations*

233 The Zn, Cd and Cu concentrations were determined in the shoots and roots of the maize. One
234 gram of shoot/root tissues was dried to a constant weight at 105 °C and then digested in a
235 mixture of HNO₃ (65%; 8 mL) and H₂O₂ (30%; 2 mL) using a Milestone Ethos One microwave
236 oven (Milestone, USA). Mineralization was performed according to the manufacturer's
237 recommendation. The total concentrations of Zn, Cd and Cu were estimated using an atomic
238 absorption spectrophotometer (ICP–OES OPTIMA 8300DV, Perkin Elmer, UK). Additionally,
239 the translocation factor (TF), defined as the metal concentration ratio of plant shoots to roots,
240 was calculated.

241

242 *2.9 Fluorescein diacetate hydrolyzing activity*

243 Fluorescein diacetate (FDA) hydrolyzing activity in soil was performed to determine the total
244 activity of soil microorganisms on days 20 and 40 of the experiment according to Sułowicz et
245 al. (2016). The concentration of free fluorescein in the filtered solution was measured at 490
246 nm using a Helios Epsilon (Thermo Fisher Scientific, Waltham, MA USA) spectrophotometer
247 and calculated in reference to the calibration curve.

248

249 *2.10 RNA extraction and RT-qPCR*

250 RNA was extracted from soils ($n = 3$ for each treatment and duration) taken on days 20 and 40
251 of the experiment using an RNeasy PowerSoil Total RNA Kit (Qiagen, Germantown, MD,
252 USA) according to the manufacturer's instructions. The quantity and quality of the RNA were
253 assessed using an Implen NanoPhotometer spectrophotometer (Implen GmbH, Munich,
254 Germany). For removal of any residual contaminating DNA from the total RNA, RQ1 RNase-
255 free DNase (Promega, Madison, WI, USA; 1 U μg^{-1} RNA for 30 min at 37 °C) was used. The
256 RevertAid First Strand cDNA Synthesis Kit (Thermo Scientific, Waltham, MA, USA) was used
257 for synthesis of the cDNA. The remaining RNA samples were stored at -80 °C. The cDNA
258 samples were stored at -20 °C.

259 Quantification of expression of the 16S rRNA gene and genes encoding the enzymes involved
260 in the degradation of hydrocarbons (alkane monooxygenase (*alkB*), alkane hydroxylase (*alkH*),
261 long-chain alkane monooxygenase (*ladA*), cytochrome P450-type alkane hydroxylase
262 (CYP153), catechol 1,2-dioxygenase (C12O) and catechol 2,3-dioxygenase (C23O)) was
263 performed in soils from the studied treatments on days 20 and 40 of the experiment using real-
264 time PCR. qPCR was conducted in triplicate using specific primer sets (Table S) (Edwards et
265 al., 1989; Phillips et al., 2008; Powell et al., 2006; Sei et al., 1999; Yousaf et al., 2010) and a
266 LightCycler 96 Real-Time PCR System (Roche Diagnostics, Florham Park, NJ, USA)
267 following the protocol described by Pacwa-Płociniczak et al. (2019).

268

269 *2.11 cDNA library preparation and RNA sequencing*

270 RNA sequencing was performed for samples extracted from the tested soils taken on day 20 of
271 the experiment. The integrity of RNA was evaluated using the Agilent 2100 Bioanalyzer
272 (Agilent Technologies, CA, USA). Ribosomal RNA depletion was performed using the
273 NEBNext rRNA Depletion Kit (Bacteria) (New England BioLabs, Germany); the library was
274 constructed using TruSeq Stranded Total RNA (Illumina, San Diego, CA, USA). The libraries

275 were sequenced using the Illumina NovaSeq 6000 (2x150 bp, paired-end, Illumina, San Diego,
276 CA, USA). The obtained data were analyzed by an integrated approach of ATLAS (a workflow
277 for assembly, annotation, and genetic binning of metagenome sequence data,
278 <https://github.com/metagenome-atlas/atlas>) (Kieser et al., 2020). Briefly, quality control of raw
279 sequences, as well as error correction based on k-mer coverage and paired-end read merging,
280 was performed using utilities in the BBTools suite, then metaSPAdes was used for *de novo*
281 assembly. For annotation, the prediction of open reading frames (ORFs) using Prodigal was
282 carried out; the translated gene products were then clustered using linclust to generate non-
283 redundant gene and protein catalogs, which were mapped to the eggNOG catalog. The
284 sequences generated in this study were deposited in the GenBank SRA database under
285 BioProject accession number PRJNA1036546.

286

287 *2.12 Taxonomic profiling*

288 KneadData (v0.12.0, <https://huttenhower.sph.harvard.edu/kneaddata/>), a pipeline of both
289 Trimmomatic (Bolger et al., 2014) and Bowtie2 (Langmead and Salzberg, 2012), was used to
290 perform quality control of metatranscriptomic sequencing data. The processed reads were then
291 used to perform the taxonomic analysis using MetaPhlan 4.0 (Blanco-Miguez et al., 2022), a
292 computational tool that aligns metagenome reads to a unique clade-specific marker-gene
293 database to perform taxonomic classification.

294

295 *2.13 Differential abundance analysis*

296 The differential abundance analysis was performed using the MaAsLin 2 (Microbiome
297 Multivariable Associations with Linear Models) package (Bioinductor) that uses a variance-
298 stabilizing arcsine square root transformation to create continuous abundance profiles that can
299 be analyzed by regular linear models (Mallick et al., 2021) employing the R software. The genes

300 with a P value (P -adj) < 0.05 and absolute fold change > 2.0 were considered as differentially
301 expressed. The Gene Ontology (GO) enrichment and Kyoto Encyclopedia of Genes and
302 Genomes (KEGG) enrichment were conducted using topGO (Alexa and Rahnenführer, 2023)
303 and clusterProfiler (Wu et al., 2021) packages, to identify the biological functions and pathways
304 affected by the differentially expressed genes (DEGs), respectively.

305

306 *2.11 Statistical analysis*

307 Statistical analysis was performed using STATISTICA 13.3 PL software (StatSoft, Tulsa,
308 USA). An analysis of variance (ANOVA) followed by Tukey's honestly significant difference
309 test (Tukey HSD test) was performed to estimate any significant effect of the individual
310 treatments on the TPH removal, total microbial activity, and the number of 16S rRNA, CYP153,
311 and *acdS* gene transcripts. Differences between treatments with $P < 0.05$ were considered
312 significant. For the experiments, data are presented as the mean \pm standard deviation (SD) of
313 three biological replicates.

314

315 *3. Results*

316 *3.1 TPH removal and heavy metal accumulation.*

317 In all experimental groups with the addition of MBM, on the 30th day after germination, the
318 plants began to show symptoms of exposure to toxic substances and finally died shortly after.
319 At the later time points, plant growth was observed only in the experimental group without
320 MBM added, indicating that adding biofertilizer at the tested concentration, but not the presence
321 of pollutants in the soil, is the reason for the toxic effect on plants. Nevertheless, the experiment
322 was continued until the end of the planned period of time.

323 The initial TPH content in the soil was 2330 ± 331 mg kg⁻¹ DW, whereas the initial
324 concentration of Zn, Cd and Cu was 2360 ± 118 ; 11.7 ± 1 and 41.5 ± 1.2

325 mg kg⁻¹ DW of soil, respectively. PH removal from soil subjected to the different treatments
 326 was estimated on days 20 and 40 after bacterial inoculation (Table 1). On day 20, significantly
 327 ($P < 0.05$) higher efficiency of hydrocarbon removal was observed in all soils enriched with
 328 MBM compared to soil without MBM added, taken from the W group, where maize plants were
 329 still alive; however, no significant ($P < 0.05$) differences in the removal efficiency were
 330 observed between soils treated with living (BL+MBM, 31.15 ± 2.22%) and thermally
 331 inactivated (TI+MBM, 32.70 ± 2.77%) cells of the ZCR6 strain and soil treated with water
 332 (W+MBM, 31.96 ± 7.18%). A similar tendency was observed on day 40; however, no further
 333 hydrocarbon removal was observed between days 20 and 40.

334

335 Table 1. TPH removal efficiency in bioremediation treatments.

Treatment	TPH removal (%)	
	20 days	40 days
BL+MBM	31.15 ± 2.22 ^a	32.02 ± 0.30 ^a
BTI+MBM	32.70 ± 2.77 ^a	33.12 ± 2.77 ^a
W+MBM	31.96 ± 7.18 ^a	34.67 ± 1.76 ^a
W	18.14 ± 1.50 ^b	19.61 ± 1.55 ^b

336 BL – live bacteria; BTI – thermally inactivated bacteria; W – water; MBM – meat and bone meal.
 337 Different letters (within each group) indicate significant differences ($P < 0.05$, Tukey test); ± Stand.
 338 Dev. of three independent experiments

339

340

341 Because plants from the treatments supplemented with MBM did not survive until the end of
 342 the experiment, the concentrations of Zn, Cd, and Cu were measured only for the control plants
 343 from the W treatment. The accumulation of these metals in non-treated maize was confirmed,
 344 but mainly in the roots, where concentrations of Zn, Cd and Cu were 1330 ± 133, 27.4 ± 6.8

345 and 32.4 ± 9.3 mg kg⁻¹ DW of plants, respectively. The tested metals' translocation factor (TF)
 346 reached values of 0.23 ± 0.02 , 0.043 ± 0.00 and 0.34 ± 0.04 , respectively (Table 2).

347

348 Table 2. Accumulation of Cd, Zn and Cu in *Z. mays* grown in the soil from treatment W.

Plant part	Heavy metal		
	Cd	Zn	Cu
roots	27.4 ± 6.8	1330.3 ± 433.1	32.4 ± 9.3
shoots	1.18 ± 0.1	300.3 ± 30.2	10.9 ± 1.1
TF	0.04 ± 0.00	0.23 ± 0.02	0.34 ± 0.04

349 TF – translocation factor; \pm Stand. Dev. of three independent experiments

350

351

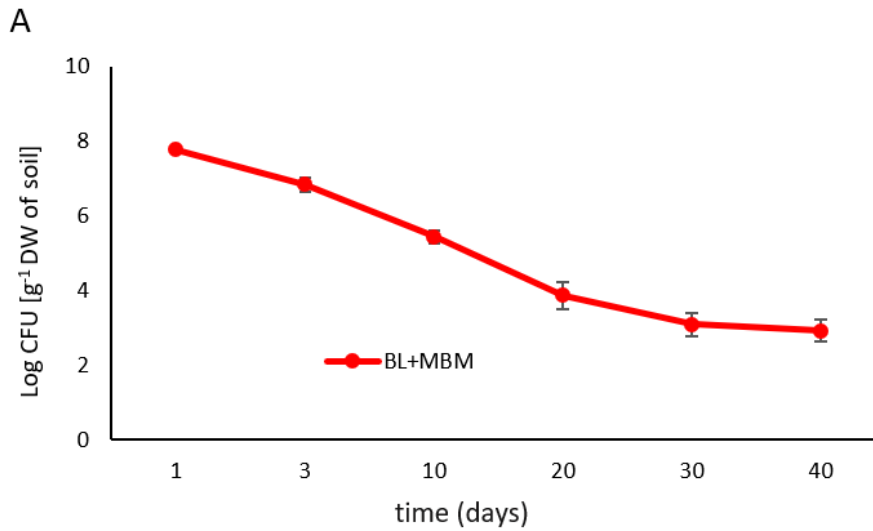
352 3.2 Fate of the ZCR6 strain in the soil

353

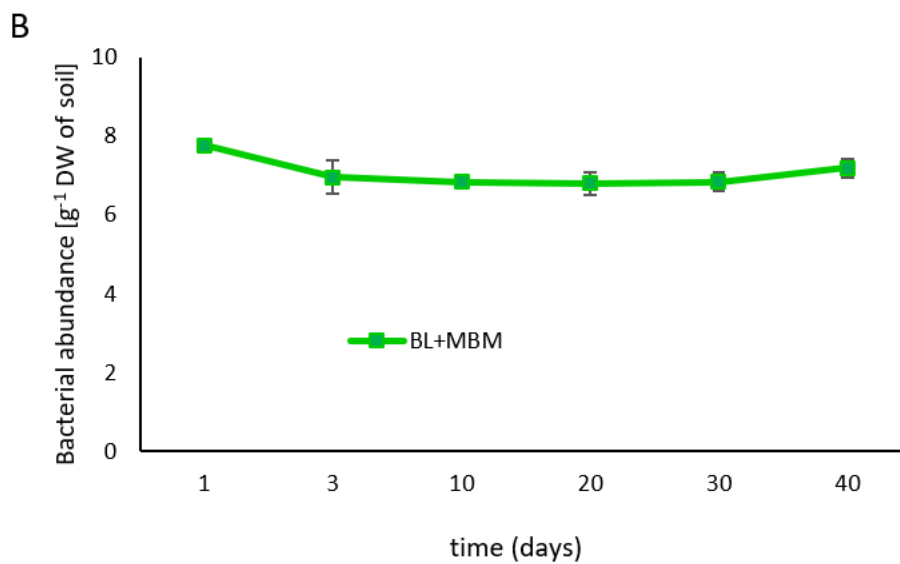
354 The rifampicin-resistant mutant of the ZCR6 strain harboring the pMP4655 plasmid vector with
 355 constitutive expression of the *egfp* gene was monitored for its ability to survive in the soil and
 356 to colonize roots and shoots of the maize after its bioaugmentation. The cells of the inoculated
 357 strain were detected in the soil until the end of the experiment using the plating method and
 358 fluorescence microscopy. The results from the dilution plate method on LB plates supplemented
 359 with rifampicin showed that three days after soil inoculation, the number of ZCR6 cells
 360 decreased one order of magnitude from the initial 7.8 to 6.8 log₁₀ cfu g⁻¹ DW of soil in treatment
 361 BL+MBM (Fig. 1a). At days 10, 20, 30 and 40 of the experiment, the number of cells decreased
 362 gradually, reaching values of 5.6, 3.4, 3.9 and 3.7 log₁₀ cfu g⁻¹ DW of soil, respectively. The
 363 results from flow cytometry analysis confirmed a decrease in the number of ZCR6 cells on day
 364 3 of the experiment to 6.9 log₁₀ cell number g⁻¹ DW of soil (Fig. 1b); however, at the following

365 sampling points, until the end of the experiment, the number of ZCR6 cells remained at a stable
366 level of approximately $6.7 \log_{10}$ cell number g^{-1} DW of soil.

367



368



369

370 Fig. 1 Number of ZCR6 strain cells detected by plating method (a) and flow cytometry (b) in
371 the soil; BL – live bacteria; MBM – meat and bone meal. The data presented are the means and
372 standard deviations (SD) of three replicates.

373

374 *3.3 Total activity of soil microorganisms*

375 The total microbial activity on days 20 and 40 of the experiment was determined by FDA
376 hydrolysis. For both sampling days, significantly ($P < 0.05$) higher microbial activity was
377 reported for all soils enriched with MBM, compared to soil not supplemented with MBM. On
378 day 20, the total activity calculated for soil BL+MBM was 9 times higher, whereas for soils
379 BTI+MBM and W+MBM it was 11 times higher, compared to soil not treated with meat and
380 bone meal. On the other hand, among treatments with MBM, soil BL+MBM was characterized
381 by significantly lower microbial activity compared with soil W+MBM. The analysis performed
382 for the samples from day 40 showed no significant differences in the activity of microorganisms
383 in all the experimental groups treated with MBM; however, the microbial activity calculated
384 for the MBM-treated soils was still about 12 higher than for soil W (Table 3).

385

386 Table 3. Total microbial activity for the soil from different treatments.

Treatment	FDA hydrolysis [μg fluorescein g^{-1} d. w.soil]	
	20 days	40 days
BL+MBM	25.99 ± 1.48^b	26.42 ± 0.39^a
BTI+MBM	31.00 ± 3.16^{ab}	24.77 ± 2.79^a
W+MBM	32.53 ± 3.36^a	26.10 ± 0.40^a
W	2.87 ± 0.83^c	2.18 ± 0.40^b

387 BL – live bacteria; BTI – thermally inactivated bacteria; W – water; MBM – meat and bone meal.
388 Different letters (within each group) indicate significant differences ($P < 0.05$, Tukey test); \pm Stand.
389 Dev. of three independent experiments

390

391

392

393

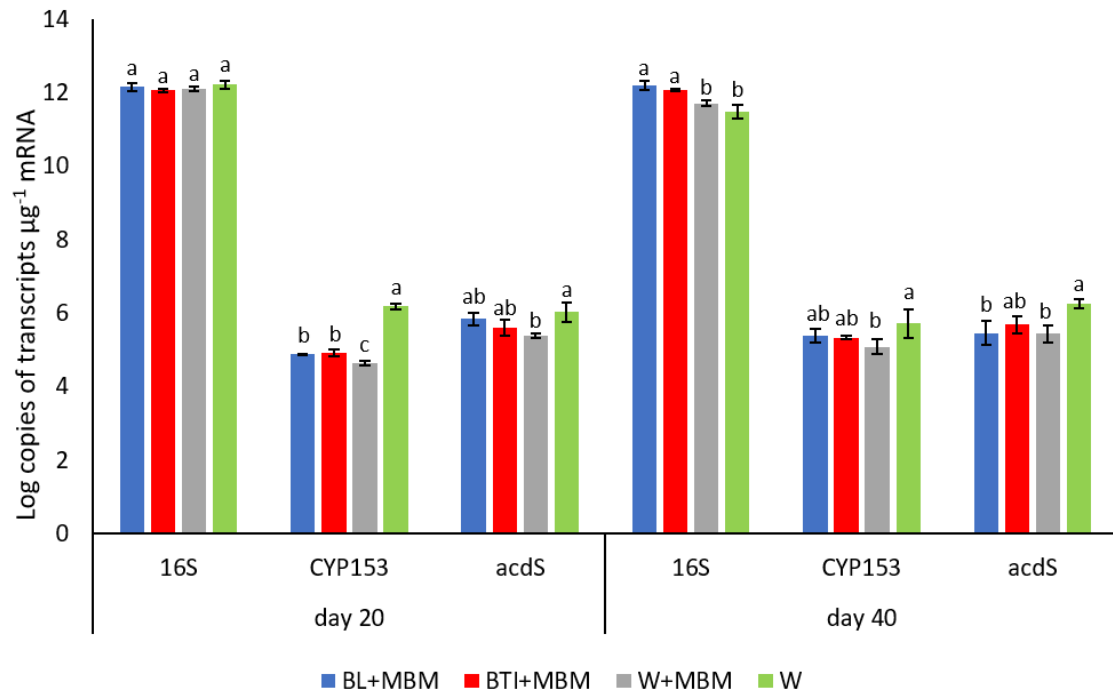
394 3.4 Quantification of gene expression levels

395 On day 20, the expression of the 16S rRNA gene in all tested samples was in the range of 12.06-
396 12.21 \log_{10} copies g^{-1} DW of soil, and no significant differences were found between treatments.
397 In turn, on day 40, the expression level of the 16S rRNA gene was significantly ($P < 0.05$)
398 higher in soils BL+MBM and BTI+MBM than in soils W and W+MBM (Fig. 2).

399 Among the tested genes involved in PH degradation, only the CYP153 gene was detected in
400 the analyzed soil. It was demonstrated that on day 20 the number of transcripts of this gene was
401 significantly ($P < 0.05$) lower in all soils supplemented with MBM than in the soil not enriched
402 with this fertilizer (20, 18, and 35 times lower in the BL+MBM, BTI+MBM and W+MBM soils
403 than in the W soil, respectively). On day 40, a significantly ($P < 0.05$) lower expression level
404 of the CYP153 gene in soils enriched with MBM compared to nonsupplemented soil was
405 detected only in the W+MBM treatment. The number of transcripts of this gene estimated in
406 the W+MBM soil was 5 times lower than that in the W soil (Fig. 2).

407 Among the tested genes involved in plant growth promotion, only the expression of the *acdS*
408 gene was observed in the tested soils. A lower number of *acdS* transcripts was also noted in
409 soils with MBM than in soil without the addition of fertilizer (W). On day 20, these differences
410 were significant ($P < 0.05$) only between soil W+MBM (5.38 \log_{10} copies g^{-1} DW of the soil)
411 and treatment W (6.02 \log_{10} copies g^{-1} DW of the soil), while on day 40, they were observed
412 between soil W (6.25 \log_{10} copies g^{-1} DW of the soil) and treatments BL+MBM (5.45 \log_{10}
413 copies g^{-1} DW of the soil) and W+MBM (5.43 \log_{10} copies g^{-1} DW of the soil) (Fig. 2).

414



415

416 Fig. 2 Number of 16S rRNA, CYP153 and *acdS* transcript copies in soils during the experiment;
 417 BL – live bacteria; BTI – thermally inactivated bacteria; W – water; MBM – meat and bone
 418 meal. The data presented are the means and standard deviations (SD) of three replicates.
 419 Different letters (within each group) indicate significant differences ($P < 0.05$, Tukey HSD-
 420 test).

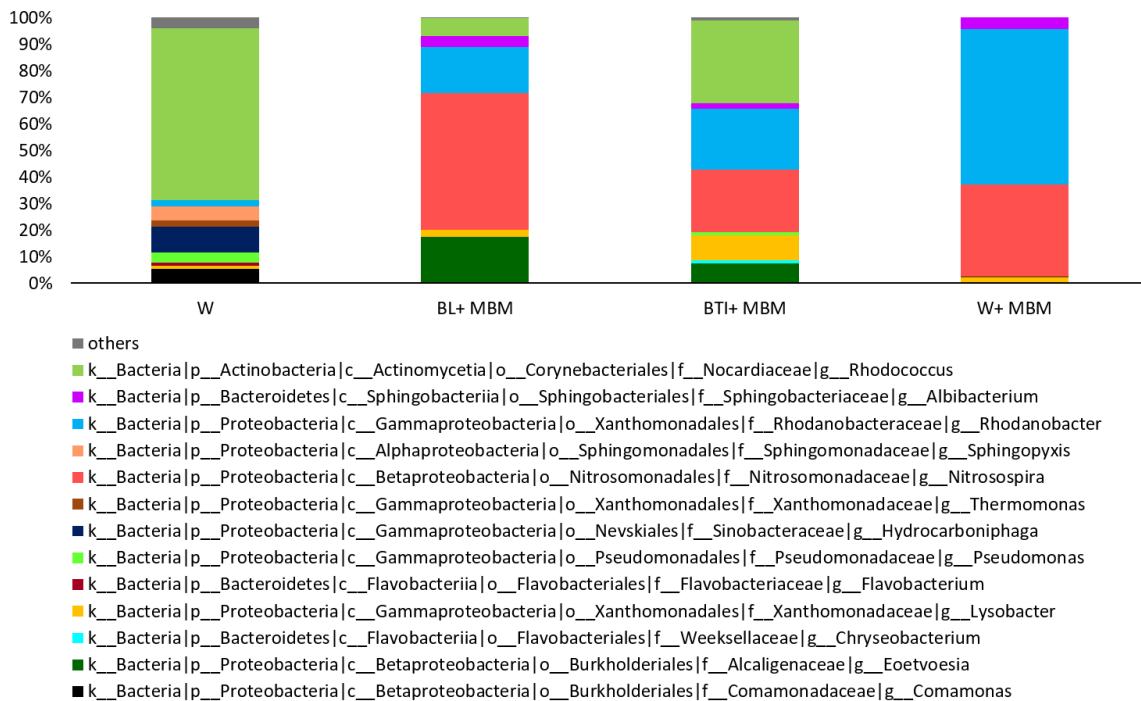
421

422 3.5 Bacterial community structure

423 The taxonomic classification performed for the cDNA sequences from day 20 of the experiment
 424 revealed that fertilization of soils with MBM changed the composition of the bacterial
 425 community, causing the appearance of *Nitrospira* and *Albibacterium* bacteria, as well as an
 426 increase in the abundance of *Rhodanobacter* and *Lysobacter* genera compared to soil W (Fig.
 427 3). Nevertheless, the abundance of the sequences characteristic for all these genera differed
 428 between MBM-treated soils. The highest abundance of *Nitrospira* was estimated for soil
 429 BL+MBM (51.48%), whereas in soils BTI+MBM and W+MBM it was 23.60% and 34.22%,
 430 respectively. For *Albibacterium* the abundance ranged between 1.94% (BTI+MBM) and about

431 4.2% (BL+MBM and W+MBM). In the case of *Rhodanobacter* the highest abundance of
 432 sequences characteristic for this genus was observed in soil W+MBM (58.67%), whereas in
 433 soils BL+MBM and BTI+MBM it reached values of 17.35% and 22.95%, respectively.
 434 Abundance of the genus *Lysobacter* reached the values of 9.44% in the soil BTI+MBM and
 435 about 2.3% in soils BL+MBM and W+MBM. In soils treated with MBM and both variants of
 436 bacteria, the presence of the genera *Rhodococcus* (6.75% for BL+MBM and 31.14% for
 437 BTI+MBM) and *Eoetvoesia* (17.51% for BL+MBM and 7.52% for BTI+MBM) was observed.
 438 Bacteria from the *Rhodococcus* genus dominated in the soil not treated with MBM, where they
 439 accounted for 64.71% of all detected bacteria, while they were not observed in the MBM+W
 440 soil. In turn, sequences characteristic for *Eoetvoesia* were not detected either in the MBM+W
 441 or in the W soil.

442



443

444 Fig. 3 Relative abundance of the bacterial genera in soils on day 20 of the experiment; W –

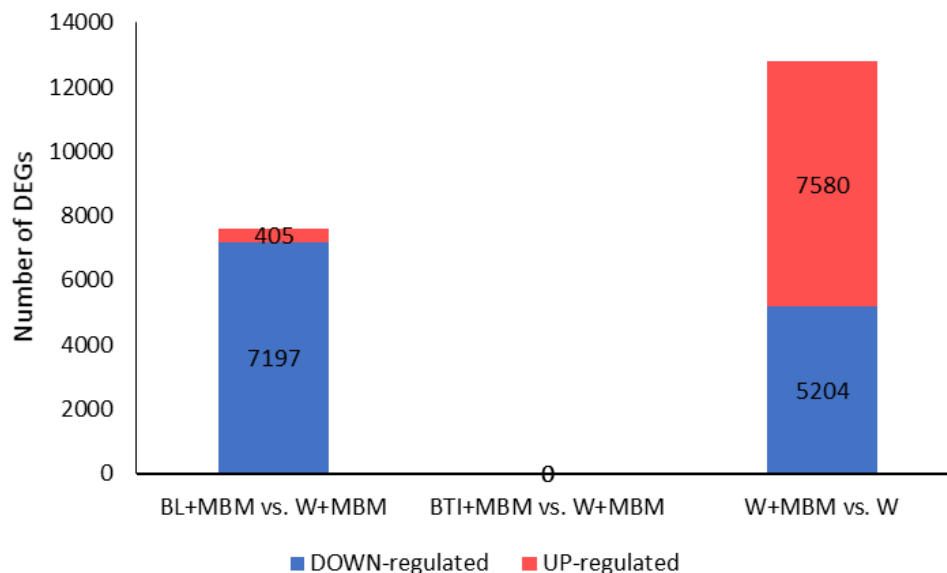
445 water; BL – live bacteria; BTI – thermally inactivated bacteria; MBM – meat and bone meal.

446

447 3.6 Differentially expressed genes detected in metatranscriptomic analysis

448 To compare the gene expression changes between treatments on day 20 of the experiment, three
449 contrast groups were established: 1) BL+MBM vs. W+MBM, 2) BTI+MBM vs. W+MBM, 3)
450 W+MBM vs. W. A comparison of BL+MBM soil with W soil revealed 7,602 (405 up- and
451 7,197 down-regulated) genes that were differentially expressed (DEGs); no DEGs were
452 detected when comparing BT+MBM versus W soil, whereas 11,095 genes (7,580 up-, and
453 5,204 down-regulated) were differentially expressed between soils W+MBM and W (Fig. 4).

454



455

456 Fig. 4 Comparative analysis of differentially expressed genes (DEGs) identified within three
457 contrast groups; BL – live bacteria; BTI – thermally inactivated bacteria; W – water; MBM –
458 meat and bone meal.

459

460 3.7. GO enrichment analysis

461 GO enrichment analysis (enrichment $p.adjust < 0.05$) of DEGs was carried out to find
462 significant GO terms (in each of the GO categories: Biological Process (BP), Cellular

463 Component (CC) and Molecular Function (MF)) specific for applied treatment on day 20 of the
464 experiment.

465 Among the significant BPs associated with up-regulated genes in the BL+MBM soil were those
466 associated with growth (GO:0040007). Among MFs the most represented were transcripts
467 related to ATP-dependent activity (GO:0140657), ATPase-coupled ion transmembrane
468 transporter activity (GO:0042625), and zymogen binding (GO:0035375). In the case of CC, the
469 most enriched functional categories were plasma membrane (GO: 0005886), cell wall
470 (GO:0005618), intracellular non-membrane-bound organelle (GO: 0043232), and cytosolic
471 large ribosomal subunit (GO:0022625) (Fig. S1).

472 The most enriched significant BPs associated with down-regulated genes in BL+MBM
473 soil were nicotinamide nucleotide metabolic process (GO:0046496), cell division
474 (GO:0051301), and protein maturation (GO:0051604). Among MFs the most enriched
475 functional categories were unfolded protein binding (GO:0051082), catalytic activity, acting on
476 a protein (GO:0140096), as well as carbamoyl-phosphate synthase (ammonia, GO:0004087),
477 and carbamoyl-phosphate synthase (glutamine-hydrolyzing, GO:0004088) activity, whereas
478 with CC the most represented were transcripts related to cytoplasm (GO:0005737), protein-
479 containing complex (GO:0032991), and membrane (GO:0016020) (Fig. S2).

480 GO enrichment analysis performed for up-regulated genes in the W+MBM soil revealed
481 the predominance of the following functional categories among BPs: ‘*de novo*’ protein folding
482 (GO:0006458) and chaperone-mediated protein folding (GO:0061077). Among MFs the most
483 enriched categories were protein folding chaperone (GO:0044183), unfolded protein binding
484 (GO:0051082), and ATP hydrolysis activity (GO:0016887), whereas among CC the most
485 represented were intracellular anatomical structure (GO:0005622), cytoplasm (GO:0005737),
486 protein-containing complex (GO:0032991), and intracellular organelle (GO:0043229) (Fig.
487 S3). On the other hand, the most significant BP associated with down-regulated genes enriched

488 in W+MBM soil was that associated with growth (GO:0040007). In the case of MFs, the most
489 enriched functional category was structural constituent of ribosome (GO:0003735), and among
490 CCs the most significant were cytosol (GO:0005829), plasma membrane (GO:0005886), cell
491 wall (GO:0005618), cytosolic small ribosomal subunit (GO:0022627), and extracellular region
492 (GO:0022627) (Fig. S4).

493

494 3.8 KEGG enrichment analysis

495 KEGG enrichment analysis (enrichment $p.adjust < 0.05$) of DEGs was performed to investigate
496 the effect of applied treatment on the pathway network in tested soil taken on day 20 of the
497 experiment. Among the significant pathways associated with up-regulated transcripts in the
498 BL+MBM soil only three pathways were indicated: caprolactam degradation, fatty acid
499 degradation and glycine, serine and threonine metabolism. In the caprolactam degradation
500 pathway, partial DEGs were involved in metabolizing cyclohexane (*alkB*, *chnB*), whereas
501 among DEGs associated with fatty acid degradation genes encoding alkane 1-monooxygenase
502 (*alkB*) and butyryl-CoA dehydrogenase (*bcd*) were detected (Fig. 5a).

503 In the case of significant pathways associated with down-regulated genes in BL+MBM soil, the
504 most represented were: biosynthesis of cofactors, biosynthesis of amino acids, and carbon
505 metabolism. In the mentioned pathways numerous DEGs were associated; nevertheless, it can
506 be summarized that down-regulated genes were involved in glycolysis [encoding fructose-
507 bisphosphate aldolase (ALDO), glyceraldehyde 3-phosphate dehydrogenase (*gapA*),
508 phosphoglycerate kinase (*pgk*), 2,3-bisphosphoglycerate-dependent phosphoglycerate mutase
509 (*gpmA*), enolase (*eno*), pyruvate kinase (*pyk*), glucose-6-phosphate isomerase (*pgi*) and 6-
510 phosphofructokinase 1 (*pfkA*)], the Entner-Doudoroff pathway [encoding glucose-6-phosphate
511 1-dehydrogenase (*zwf*), 6-phosphogluconolactonase (*pgl*), phosphogluconate dehydratase
512 (*edd*)], pyruvate oxidation [encoding pyruvate dehydrogenase E1 component (*aceE*)], citrate

513 cycle [encoding aconitate hydratase (*acnA*), isocitrate dehydrogenase (*icd*), 2-oxoglutarate
514 dehydrogenase E1 component (*sucA*), succinyl-CoA synthetase alpha subunit (*sucD*), succinate
515 dehydrogenase flavoprotein subunit (*sdhA*), fumarate hydratase (*fumA*), malate dehydrogenase
516 (MDH1) and citrate synthase (*gltA*)], as well as the pentose phosphate pathway (encoding
517 glucose-6-phosphate 1-dehydrogenase (*zwf*), 6-phosphogluconolactonase (*pgl*), 6-
518 phosphogluconate dehydrogenase (*gnd*), glucose-6-phosphate isomerase (*pgi*), transaldolase
519 (*talB*), fructose-bisphosphate aldolase (ALDO), transketolase (*tktA*), ribose 5-phosphate
520 isomerase A (*rpiA*), and ribulose-phosphate 3-epimerase (*rpe*)]. The other significant down-
521 regulated pathways in BL+MBM soil were related to oxidative phosphorylation, ribosome,
522 metabolism of amino acids (cysteine, methionine, glycine, serine, threonine, alanine, aspartate,
523 glutamate), pyruvate, propanoate, glyoxylate, dicarboxylate, and lipoic acid, as well as bacterial
524 secretion system, biosynthesis of aminoacyl-tRNA, fatty acid, and amino acids (valine, leucine
525 and isoleucine), and protein export. Down-regulated DEGs involved in the bacterial secretion
526 system included genes associated with secretion system Type I [encoding outer membrane
527 protein (*tolC*)], Type II [encoding general secretion pathway protein D (*gspD*), general
528 secretion pathway protein G (*gspG*) and general secretion pathway protein H (*gspH*)], Type VI
529 [encoding type VI secretion system secreted protein Hcp (*hcp*), ImpL (*impL*), and VasG
530 (*vasG*)], secretion system Sec-SRP [encoding preprotein translocase subunit SecD (*secD*),
531 SecG (*secG*), SecY (*secY*), and YajC (*yajC*), YidC/Oxa1 family membrane protein insertase
532 (*yidC*), fused signal recognition particle receptor (*ftsY*), preprotein translocase subunit SecA
533 (*secA*), and SecB (*secB*), and signal recognition particle subunit SRP54 (*ffh*)], as well as Twin
534 arginine targeting (Tat) secretion system [encoding sec-independent protein translocase protein
535 TatA (*tatA*), TatB (*tatB*), TatC (*tatC*) and TatE (*tatE*)] (Fig. 5a)

536 KEGG enrichment analysis of DEGs in the W+MBM soil revealed that among the most
537 significant pathways associated with up-regulated genes were biosynthesis of cofactors,

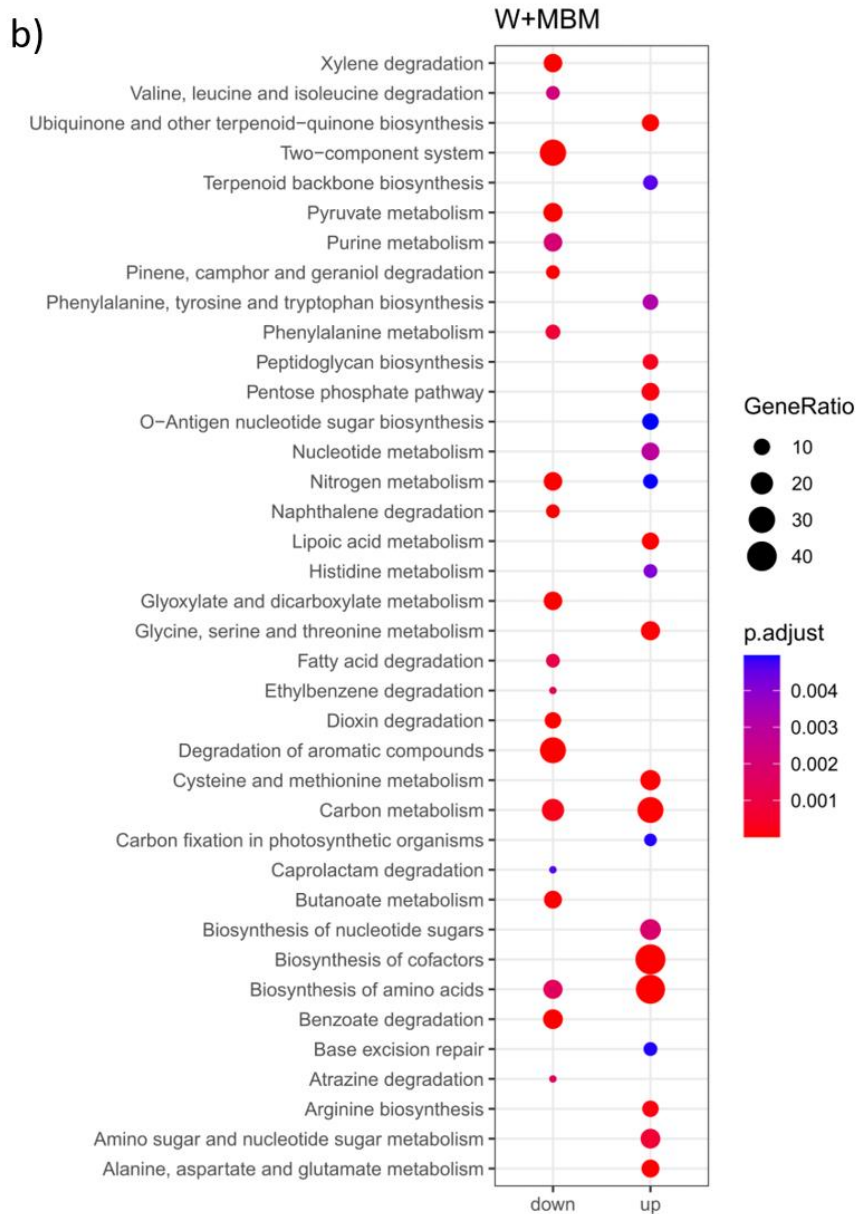
538 biosynthesis of amino acids, and carbon metabolism. Among DEGs involved in carbon
539 metabolism up-regulated genes were associated with methane oxidation [encoding
540 methane/ammonia monooxygenase subunit A (*pmoA-amoA*)], glycolysis [*pgi*, *pfkA*, ALDO,
541 *gpmA*], pyruvate oxidation [*aceE*], and the pentose phosphate pathway [*pgi*, *talB*, *rpiA*]. The
542 other significant up-regulated pathways in W+MBM soil were associated with biosynthesis of
543 nucleotide sugars, ubiquinone and other terpenoid-quinones, amino acids, O-antigen nucleotide
544 sugars, the peptidoglycan and terpenoid backbone, metabolism of amino acids, amino sugars,
545 nucleotide sugars, nucleotides, lipoic acid, and nitrogen, as well as degradation of amino acids,
546 base excision repair and carbon fixation in photosynthetic organisms. Among up-regulated
547 genes related to nitrogen metabolism were those associated with nitrification [*pmoA-amoA*, and
548 *hao* (encoding hydroxylamine dehydrogenase)], and partially with denitrification (encoding
549 nitric oxide reductase subunit B (*norB*)) (Fig. 5b). Among significantly down-regulated
550 pathways the most represented were related to the two-component system, degradation of
551 aromatic compounds and the carbon system. Additionally, in the W+MBM soils down-
552 regulated genes were also associated with degradation of different compounds (i.e. benzoate,
553 xylene, dioxin, naphthalene, fatty acids, amino acids, ethylbenzene, atrazine, and caprolactam),
554 metabolism of pyruvate, nitrogen, glyoxylate, dicarboxylate, purine, butanoate, and
555 phenylalanine, as well as biosynthesis of amino acids. Among down-regulated DEGs involved
556 in nitrogen metabolism were genes related to dissimilatory nitrate reduction [encoding nitrate
557 reductase/nitrite oxidoreductase, alpha subunit (*narG*), nitrate reductase (*napA*), nitrite
558 reductase (NADH) large subunit (*nirB*)], denitrification [*narG*, *napA* and *nirS* (encoding nitrite
559 reductase (NO-forming)/hydroxylamine reductase)], and related to the last step of nitrification
560 (*narG*) and the first step of anammox (*nirS*). Moreover, genes encoding nitronate
561 monooxygenase (NMO), the NNP family, nitrate/nitrite transporter (*nark*), nitrate/nitrite
562 transport system substrate-binding protein (*nrtA*) and hydroxylamine reductase (*hcp*) were

563 down-regulated. It was observed that some of the pathways were associated with both up- and
 564 down-regulated DEGs; nevertheless, within a given pathway, some processes were up- while
 565 others were down-regulated (Fig. 5b).

566



567



568

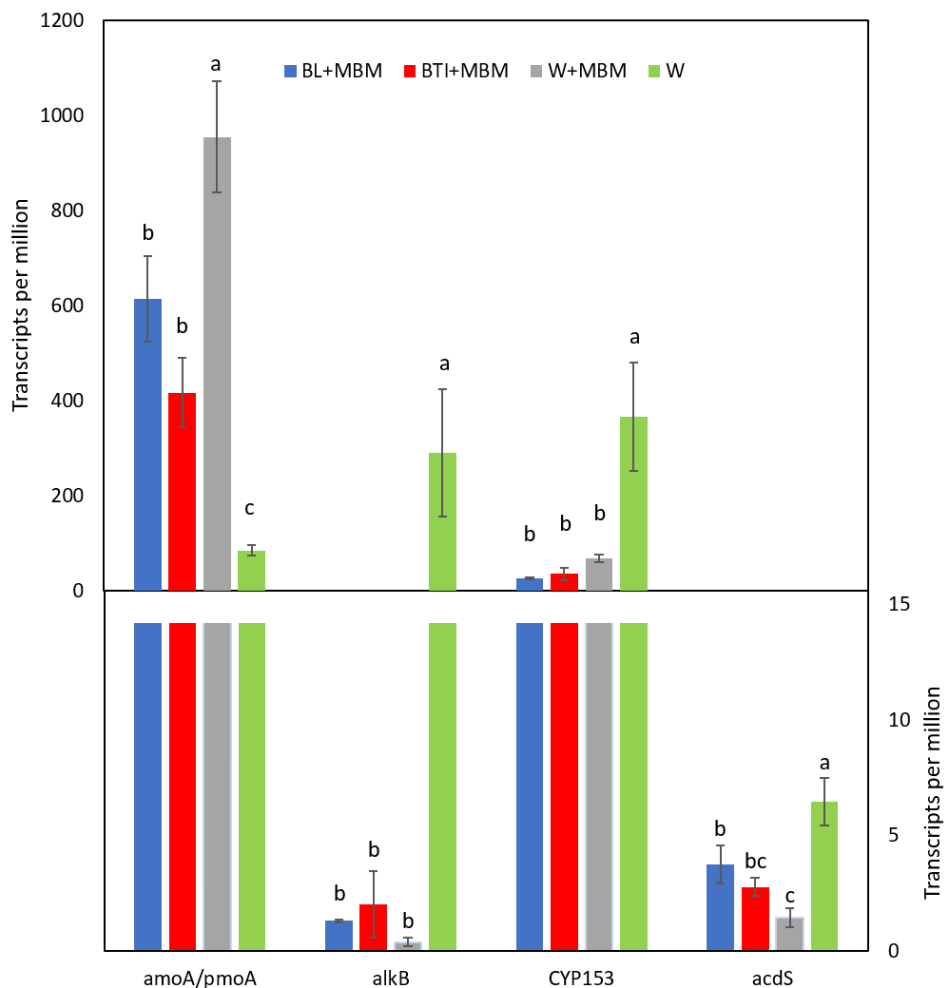
569 Fig. 5 KEGG enrichment analysis of Differentially Expressed Genes (DEGs) in response to
 570 BL+MBM (a) and W+MBM (b) treatments; BL – live bacteria; W – water; MBM – meat and
 571 bone meal.

572

573 *3.9 Transcription of selected genes crucial for phytoremediation efficiency*

574 The abundance of hydrocarbon degradation-related gene transcripts, as well as transcripts of
 575 ACC deaminase gene, was studied (Fig.6). Within the group of genes associated with PH

576 degradation, expression of *pmoA-amoA*, encoding methane particulated ammonia
 577 monooxygenase subunit A, CYP153, encoding cytochrome P450 alkane hydroxylase 1, and
 578 *alkB*, encoding alkane 1-monooxygenase, was reported in all tested soils. Expression of the
 579 mentioned genes differed between treatments, and a significantly higher number of *pmoA-amoA*
 580 transcripts (417-954 reads per million, rpm) was observed in soils amended with MBM,
 581 compared to soil W (85 rpm). In turn, in soil non-treated with MBM, the significantly higher
 582 abundance of CYP153 (365 rpm) and *alkB* (290 rpm) transcripts was revealed, compared to
 583 MBM soils (26-68 rpm for CYP153, and 0.4-2 rpm for *alkB*). In the case of *acdS* gene, a low
 584 number of transcripts (max. 6 rpm) was estimated in all tested soils.



585
 586 Fig. 6 Abundance of transcripts of *pmoA-amoA*, *alkB*, CYP153 and *acdS* gene. BL – live
 587 bacteria; BTI – thermally inactivated bacteria; W – water; MBM – meat and bone meal.

588 *Discussion*

589 To the best of our knowledge, the current study is the first attempt to combine the remediation
590 capacity of a fast-growing plant (maize), a multi-way supporting PGPR strain (*Pseudomonas*
591 *qingdaonensis* ZCR6), and the addition of a slow-release fertilizer (MBM) to clean up soil
592 historically co-contaminated with PHs and HMs. A further novelty of our study is the use of
593 whole metatranscriptomics analysis for a better understanding of ongoing processes during
594 applied treatments. Even though our goal was to investigate the simultaneous use of
595 bioaugmentation and biostimulation to support the phytoremediation of co-polluted areas, due
596 to a more accessible interpretation of the obtained results, we decided to divide the discussion
597 into two subsections, each focusing separately on the treatment used.

598

599 *Consequences of the bioaugmentation for the remediation process*

600 In the laboratory, the ZCR6 strain expressed the activity of several mechanisms crucial to
601 promote plant growth, and thus potentially supporting the phytoremediation of co-contaminated
602 soil. Despite its promising characteristics, we did not observe a positive effect of the living cells
603 of the ZCR6 strain on the phytoremediation efficiency of soil contaminated with PH and HM
604 treated with MBM. Such a positive effect of the ZCR6 strain was observed earlier in our
605 preliminary tests using maize and single pollutant-containing soil (data not shown). Similar
606 observations reported previously by Liu et al. (2021) were explained as a result of the low
607 survival of the endophytic bacterial strain after its inoculation into the soil. It is well known that
608 the most important factors influencing the efficiency of bioaugmentation during bacterial-
609 assisted phytoremediation include the survival of the introduced bacteria after soil inoculation,
610 their ability to multiply in the soil, and their metabolic activity in such environment (Płociniczak
611 et al., 2017). In survival studies using plating and flow cytometry techniques, we recorded a
612 one-order-of-magnitude reduction in ZCR6 strain abundance directly after introduction into the

613 soil; which means that the number of CFU of the ZCR6 strain was reduced by 90%. This is a
614 frequent observed tendency in bioaugmentation experiments in which the fate of inoculants is
615 monitored. Most of the bacteria did not survive the soil inoculation, but still they could support
616 the plants in two ways, mainly because the bacterial necromass enhanced the pool of nutrients
617 in the soil and through the metabolic activity of the remaining 10% of inoculants. This was a
618 similar effect to that caused by the thermally inactivated strain. However, it is an open question
619 whether the remaining 10% of bacteria is a sufficient number of cells to cause a visible effect
620 detected as increased efficiency of this process. Another issue is to determine whether the
621 survived inoculants and/or indigenous bacteria showed the activity of beneficial mechanisms
622 supporting phyto- and bio-remediation of co-contaminated areas. This was analyzed using RT-
623 qPCR and metatranscriptomics techniques.

624 In the current study, we quantified the expression level of several PGP genes, but only the
625 expression of the *acdS* gene, encoding ACC deaminase, was detected in soils. However,
626 metatranscriptomic analysis revealed its expression at a minimal level, which indicates a
627 marginal impact on conducted processes. The higher abundance of *acdS* gene transcripts in W
628 soil may be related to the fact that the plants survived in this experimental group until the end
629 of the experiment and thereby could shape the composition of rhizosphere microorganisms.

630 Based on the results regarding the survival of the strain and the expression of selected PGP
631 mechanisms in the soil, we suspect that the introduced strain, due to adverse environmental
632 conditions, gradually shifted into the VBNC (viable but non-culturable) state (Su et al., 2019).

633 In this state, bacteria partially reduce their metabolism, which may reduce the activity of
634 selected metabolic pathways and cause difficulties in their cultivation on microbiological
635 media, especially supplemented with selective factors. Since rifampicin is not present in the
636 soil at concentrations that require the activation of bacterial resistance mechanisms to this
637 antibiotic, the growth of inoculants on media with high ($100 \mu\text{g mL}^{-1}$ of medium) Rif content

638 may be additionally constricted. Because the method of determining the number of inoculants
639 using flow cytometry does not require their cultivation on a selective medium, the number of
640 the EGFP-marked ZCR6 cells was significantly higher and remained constant until the end of
641 the experiment. The higher decrease in the number of rifampicin-resistant cells of the ZCR6
642 strain detected in the later phase of the experiment compared to EGFP-marked cells supports
643 such a statement.

644 Another factor that may have an impact on the efficiency of phytoremediation is additional soil
645 fertilization by dead bacteria. Bacterial necromass, being an additional source of energy and
646 carbon, is thought to serve as a biofertilizer that leads to increased activity of autochthonous
647 hydrocarbon-degrading microorganisms for a short time (Liang et al., 2019). Nevertheless, such
648 an effect was not observed in our experiment. It has been assumed that soil fertilization with
649 MBM played a crucial role in supporting the microbial degradation of PHs. This was also
650 confirmed by the significantly higher loss of PHs in MBM treatments compared to the untreated
651 control.

652 An interesting finding from the RT-qPCR analysis is that among tested genes involved in
653 hydrocarbon degradation, only the CYP153 gene was expressed in soil. Surprisingly, it was at
654 a significantly higher level in soil not enriched with MBM than in soils supplemented with this
655 fertilizer. Moreover, PH removal was higher in MBM soils. Since there was no difference in
656 PH removal between living bacteria and necromass treatments in MBM soils, introduced living
657 cells of *P. qingdaonensis* ZCR6 obviously did not contribute to the removal of hydrocarbons
658 from soil. This is not surprising, as microbial degraders often underperform *in situ* compared
659 with laboratory conditions (Bodor et al., 2021). Notably, since the *alkB*, *alkH*, C120, and C230
660 genes were not expressed in the studied soils, we assume that the degradation of hydrocarbons
661 was the effect of the activity of enzymes characteristic for autochthonous soil microorganisms,
662 which have not been tested in this study. Therefore, to better understand the mechanisms of

663 hydrocarbon decomposition in the analyzed soils, a metatranscriptomic analysis was
664 performed. The varied expression of CYP153, *alkB*, and *pmoA-amoA* was revealed in all tested
665 soils. Metatranscriptomics showed the presence of *alkB* gene transcripts in the soil, which was
666 contrary to the findings from the RT-qPCR; however, observed differences may be because the
667 used primer pair captured only part of the analyzed gene, which was also reported by Frostegård
668 et al. (2022). In the W soil, hydrocarbon degradation was mainly driven by cytochrome P450
669 alkane hydroxylase 1, and alkane 1-monooxygenase. In turn, in MBM-supplemented soils,
670 higher expression of methane particulated ammonia monooxygenase subunit A (*pmoA-amoA*)
671 by bacteria from the order *Nitrosomonadales* was reported. These integral membrane proteins
672 have a relatively wide substrate specificity and can oxidize a broad range of substrates. It can
673 catalyze oxidation of both ammonia, methane, alkyl, aryl and halogenated hydrocarbons and
674 even aromatic compounds (Arp et al., 2002). This observation suggests the important role of
675 these enzymes in the oxidation process in MBM soils. The higher expression level of *pmoA-*
676 *amoA* in soils supplemented with MBM was correlated with the changes in the bacterial
677 community composition, observed as increased abundance of bacteria from the order
678 *Nitrosomonadales* in these soils. Additionally, in MBM soils, expression of cytochrome P450
679 alkane hydroxylase 1 and alkane 1-monooxygenase was detected at a low level, which suggests
680 that these enzymes did not significantly contribute to the hydrocarbon removal process. In turn,
681 a high abundance of *pmoA-amoA* gene transcripts in MBM soils indicated its crucial role in PH
682 removal.

683

684 *Effect of MBM biofertilizer on remediation efficiency*

685 Unpredictable interactions among different types of pollutants bring more challenges to plant
686 growth or even survival; therefore, the appropriate intensification of phytoremediation helps to
687 overcome these limitations. In addition to the introduction of PGPB, the amendment of soil

688 with fertilizers can significantly increase plant biomass production and soil microbial activity
689 (Cao et al., 2022; Shtangeeva et al., 2004); therefore, in our experiment, we studied the impact
690 of MBM addition on phytoremediation efficiency. The enrichment of soil co-contaminated with
691 PHs and HMs with MBM had a negative effect on the growth of maize plants, which, however,
692 at this stage of research does not completely exclude its usefulness in supporting this process,
693 and lower concentrations of MBM should also be tested. A possible explanation for the plant
694 dieback is the increased toxicity caused by the rapid release of a large amount of ammonia from
695 the MBM, and its further transformation into highly toxic nitrites. This assumption is supported
696 by the metatranscriptomic results showing increased expression of methane/ammonia
697 monooxygenase subunit A (AMO) and hydroxylamine dehydrogenase (HAO) observed in all
698 soils fertilized with MBM. These two enzymes are involved in two-step oxidation of NH_3 ;
699 AMO catalyzes the oxidation of NH_3 to NH_2OH , and HAO catalyzes further oxidation to NO_2 .
700 Freichs et al. (2020) observed that a short time after germination seedlings of basil were
701 suffering from high NH_3 and NH_4^+ exposure caused by rapid ammonification after addition of
702 plant available N as amino acid fertilizer manufactured from enzymatically hydrolyzed animal
703 proteins. In their study strong inhibition of development of the radicle, hypocotyl, and
704 cotyledons of basil was observed. Similarly, adverse effects of ammonical N forms on
705 germination and seedling development have also been reported for cucumber, wheat, rye,
706 barley, maize and rice (Bremner and Krogmeier, 1989; Ells et al., 1991; Qi et al., 2012).
707 Despite the toxic effect of MBM on plant growth in co-contaminated soil, its positive influence
708 on the PH degradation rate *via* indigenous microorganisms in the soil was confirmed in our
709 experiment. The assumption is that MBM releases nutrients that enhance the degradation of
710 organic contaminants in mild climatic conditions (Liu et al., 2019; Sun et al., 2018). Similarly
711 to Liu et al. (2019), we found that the MBM stimulation effect was particularly evident in the
712 early remediation phase. It thus seems that MBM addition as a source of nutrients to PH

713 contaminated soil is a better strategy than the use of maize. Nevertheless, since phytoextraction
714 is the only biological method used to permanently remove HMs from soil, it is not possible to
715 abandon the use of plants in the remediation of co-contaminated areas. However, based on our
716 results, phytoremediation of co-contaminated soils should not be started simultaneously with
717 MBM application. Instead, the plant (e.g., maize) cultivation a few months after soil
718 biofertilization with MBM could lead to optimal remediation of co-contaminated soils. In such
719 an approach the MBM would stimulate microbial activity and enhance PH degradation, and
720 then plants would take up HMs and support PH rhizodegradation from pre-cleaned soil without
721 suffering from the excess of N-rich components and potential toxic products of PH degradation.
722 Despite the difficulties in using MBM in our research, the usefulness of this biofertilizer has
723 been confirmed previously. In the study of Mondini et al. (2008), the amendment of arable soils
724 with MBM caused an overall increase in the activity of soil microorganisms (determined based
725 on the hydrolysis of FDA), indicating an enhanced capacity of the soil for element cycling and
726 an improvement of its quality. An increase in FDA hydrolysis also directly indicates an
727 enhanced ability of the soil to degrade and transform organic substrates and pollutants
728 (Sánchez-Monedero et al., 2008), which is convergent with our results. Nevertheless, we also
729 observed significant differences in the microbial activity between MBM-treated soils. Lower
730 FDA hydrolysis was reported for BL+MBM soil compared to W+MBM soil. Effective
731 bioaugmentation, except for successful soil colonization, also depends on the interaction
732 between inoculants and autochthonous microorganisms. Because most of the soil bacteria are
733 unculturable, estimating such dependencies in laboratory conditions is impossible. In our
734 experiment, the ZCR6 inoculation resulted in lower soil microbial activity compared to non-
735 inoculated soil. Similarly, in the experimental group without MBM, the soil bioaugmentation
736 with live ZCR6 strain caused an even higher reduction of resulted in reduced microbial activity,
737 estimated on the level of $0.87 \mu\text{g fluorescein g}^{-1} \text{ DW}$ of soil and was 30 times lower compared

738 to soil BL+MBM (data not shown). The confirmation for this also comes from the
739 metatranscriptomic results showing significantly lower expression of genes involved in
740 glycolysis, the Entner-Doudoroff pathway, pyruvate oxidation, and the pentose phosphate
741 pathway observed in BL+MBM treatment, as compared with the number of their transcripts in
742 W+MBM soil. Moreover, decreased expression of genes encoding proteins constituting part of
743 secretion systems (Type II, Type VI, Sec-SRP), a multi-protein complex used by bacteria to
744 move substances across their cell membrane, was observed in soil BL+MBM, compared to soil
745 W+MBM. Since these systems are associated with the secretion of many diverse substrates
746 involved in bacterial adhesion, biofilm formation, and *quorum sensing* (Naskar et al., 2021),
747 they have an important role in bacterial communication (Pena et al., 2019). Thus, decreased
748 expression of genes encoding secretion systems could consequently lead to impaired
749 interactions between bacteria acting as whole communities.

750 In our experiment, we noted significantly higher hydrocarbon degradation in all soils enriched
751 with MBM, independently of the soil treatment (BL, BTI, and W), even though the plants were
752 only able to survive in this soil for 10 days and did not support this process in the most
753 experimental period. This result also indicated that hydrocarbon removal from soil co-
754 contaminated with PHs and HMs supplemented with MBM resulted mainly from the enhanced
755 activity of autochthonous microorganisms, biostimulated by the MBM addition. Such
756 observations are consistent with results from our previous studies on the bioaugmentation of
757 soil contaminated only with hydrocarbons, in which further PH loss was also noted after the
758 death of the inoculants (Pacwa-Płociniczak et al., 2019). We also reported the lack of
759 correlation between PH removal efficiency and microbial activity measured by FDA
760 hydrolysis. The FDA decomposition is a consequence of the metabolic activity of all soil
761 microorganisms (inoculants, indigenous bacteria, fungi, etc.), and only part of them is involved
762 in hydrocarbon degradation. Moreover, the changes in microbial community composition may

763 unpredictably influence the microbial activity and PH removal, which was observed in the
764 ZCR6 bioaugmented soil, non-treated with MBM, in which hydrocarbon loss reached a value
765 of 7.95% (data not shown).

766 The analysis of plants from non-treated W soil showed a limited potential of maize to remove
767 Cd, Zn, and Cu from the soil in the presence of PHs, with the highest accumulation capacity for
768 Zn. Nevertheless, the translocation factor calculated for all tested HMs was far from the value
769 of 1 desired for plants used in phytoextraction. However, the large biomass of maize and its
770 extensive root system, compared to the most effective hyperaccumulators, can compensate for
771 the lower ability to accumulate metals compared to hyperaccumulating plants. Also, the low
772 translocation factor for Cd, Zn, and Cu does not disqualify these plants, because most of the
773 roots can be removed together with aboveground parts using typical agricultural equipment,
774 and similar results confirming these features of maize were also observed in other studies on
775 phytoextraction of HMs from co-contaminated soils (Hechmi et al., 2013; Lin et al., 2008;
776 Nwosu et al., 2018; Zhang et al., 2009).

777

778

779 *5. Conclusions*

780 Although our research did not confirm the usefulness of MBM at the tested concentration to
781 support phytoremediation of co-contaminated soil, we demonstrated the potential of its use to
782 support the removal of petroleum hydrocarbons by microbial degradation. This was confirmed
783 by metatranscriptomics, which showed increased expression of genes encoding enzymes
784 potentially involved in the removal of hydrocarbons in MBM-treated soils. Our results provide
785 a rationale to perform further phytoremediation tests using a lower amount of MBM and/or soil
786 pre-treated with MBM. This approach will avoid toxic effects of high ammonia concentration
787 on plants and will enable effective removal of HMs by phytoextraction and PHs by

788 rhizodegradation due to autochthonous microorganisms. Our findings indicate that optimal
789 biofertilization of co-contaminated soil can effectively replace expensive and time-consuming
790 soil bioaugmentation with bacterial strains, such as ZCR6. Since the number of remediation
791 methods to clean up co-contaminated areas is limited, further research on the optimization of
792 phytoremediation is strongly recommended.

793

794 *Acknowledgements*

795 MP-P would like to thank Patrycja Niemiec for help with the fluorescein diacetate hydrolyzing
796 activity measurement.

797

798 *Funding*

799 This work was supported by the National Science Centre (Poland) (grant No.
800 2018/31/D/NZ9/01610).

801

802 *CRediT author statement*

803 **Magdalena Pacwa-Plociniczak:** Conceptualization, Data curation, Formal analysis, Funding
804 acquisition, Investigation, Methodology, Project administration, Resources, Software,
805 Supervision, Validation, Visualization, Writing original draft, Writing – review & editing;
806 **Agata Kumor:** Investigation; **Marta Bukowczan:** Investigation; **Aki Sinkkonen:**
807 Conceptualization, Formal analysis, Methodology, Supervision, Validation, Writing original
808 draft; **Marja Roslund:** Formal analysis, Software; **Tomasz Plociniczak:** Investigation,
809 Methodology, Writing original draft.

810

811

812 *References*

813 Alexa, A., Rahnenführer, J., 2023. Gene set enrichment analysis with topGO.

814 Arp, D.J., Sayavedra-Soto, L.A., Hommes, N.G., 2002. Molecular biology and biochemistry of ammonia
815 oxidation by *Nitrosomonas europaea*. Arch Microbiol. [https://doi.org/10.1007/s00203-002-](https://doi.org/10.1007/s00203-002-0452-0)
816 0452-0

- 817 Blanco-Miguez, A., Beghini, F., Cumbo, F., McIver, L.J., Thompson, K.N., Zolfo, M., Manghi, P., Dubois,
818 L., Huang, K.D., Thomas, A.M., Piccinno, G., Piperni, E., Punčochář, M., Valles-Colomer, M., Tett,
819 A., Giordano, F., Davies, R., Wolf, J., Berry, S.E., Spector, T.D., Franzosa, E.A., Pasolli, E., Asnicar,
820 F., Huttenhower, C., Segata, N., 2022. Extending and improving metagenomic taxonomic
821 profiling with uncharacterized species with MetaPhlan 4. bioRxiv.
822 <https://doi.org/10.1101/2022.08.22.504593>
- 823 Bloemberg, G. V., Wijnjes, A.H.M., Lamers, G.E.M., Stuurman, N., Lugtenberg, B.J.J., 2000.
824 Simultaneous imaging of *Pseudomonas fluorescens* WCS365 populations expressing three
825 different autofluorescent proteins in the rhizosphere: New perspectives for studying microbial
826 communities. *Molecular Plant-Microbe Interactions* 13, 1170–1176.
827 <https://doi.org/10.1094/MPMI.2000.13.11.1170>
- 828 Bodor, A., Bounedjoum, N., Feigl, G., Duzs, Á., Laczi, K., Szilágyi, Á., Rákhely, G., Perei, K., 2021.
829 Exploitation of extracellular organic matter from *Micrococcus luteus* to enhance ex situ
830 bioremediation of soils polluted with used lubricants. *J Hazard Mater* 417, 125996.
831 <https://doi.org/10.1016/J.JHAZMAT.2021.125996>
- 832 Bolger, A.M., Lohse, M., Usadel, B., 2014. Trimmomatic: a flexible trimmer for Illumina sequence
833 data. *Bioinformatics* 30, 2114–2120. <https://doi.org/10.1093/bioinformatics/btu170>
- 834 Bremner, J.M., Krogmeier, M.J., 1989. Evidence that the adverse effect of urea fertilizer on seed
835 germination in soil is due to ammonia formed through hydrolysis of urea by soil urease
836 (biuret/phenylphosphorodiamidate), *Proc. Nall. Acad. Sci. USA*.
- 837 Cao, X., Cui, X., Xie, M., Zhao, R., Xu, L., Ni, S., Cui, Z., 2022. Amendments and Bioaugmentation
838 Enhanced Phytoremediation and Micro-ecology for PAHs and Heavy Metals Co-contaminated
839 Soils. *J Hazard Mater* 426, 128096. <https://doi.org/10.1016/j.jhazmat.2021.128096>
- 840 Chaukura, N., Muzawazi, E.S., Katengeza, G., Mahmoud, A.E.D., 2022. Remediation technologies for
841 contaminated soil systems, in: *Emerging Contaminants in the Terrestrial-Aquatic-Atmosphere*
842 *Continuum: Occurrence, Health Risks and Mitigation*. Elsevier, pp. 353–365.
843 <https://doi.org/10.1016/B978-0-323-90051-5.00019-5>
- 844 Chirakkara, R.A., Cameselle, C., Reddy, K.R., 2016. Assessing the applicability of phytoremediation of
845 soils with mixed organic and heavy metal contaminants. *Rev Environ Sci Biotechnol* 15, 299–
846 326. <https://doi.org/10.1007/s11157-016-9391-0>
- 847 Chlebek, D., Pinski, A., Żur, J., Michalska, J., Hupert-Kocurek, K., 2020. Genome Mining and Evaluation
848 of the Biocontrol Potential of *Pseudomonas fluorescens* BRZ63, a New Endophyte of Oilseed
849 Rape (*Brassica napus* L.) against Fungal Pathogens. *Int J Mol Sci* 21, 8740.
850 <https://doi.org/10.3390/ijms21228740>
- 851 Chlebek, D., Płociniczak, T., Gobetti, S., Kumor, A., Hupert-Kocurek, K., Pacwa-Płociniczak, M., 2022.
852 Analysis of the Genome of the Heavy Metal Resistant and Hydrocarbon-Degrading Rhizospheric
853 *Pseudomonas qingdaonensis* ZCR6 Strain and Assessment of Its Plant-Growth-Promoting Traits.
854 *Int J Mol Sci* 23, 214. <https://doi.org/10.3390/ijms23010214>
- 855 Edwards, U., Rogall, T., Blöcker, H., Emde, M., Böttger, E.C., 1989. Isolation and direct complete
856 nucleotide determination of entire genes. Characterization of a gene coding for 16S ribosomal
857 RNA. *Nucleic Acids Res* 17, 7843–7853. <https://doi.org/10.1093/nar/17.19.7843>

- 858 Eils, J.E., Mesay, A.E., Workman, S.M., 1991. Toxic Effects of Manure, Alfalfa, and Ammonia on
859 Emergence and Growth of Cucumber Seedlings, HORTSCIENCE.
- 860 FAO, 2015. World reference base for soil resources 2014. Update 2015., World Soil Resources
861 Reports. <https://doi.org/10.1038/nnano.2009.216>
- 862 Frerichs, C., Daum, D., Pacholski, A.S., 2020. Ammonia and Ammonium Exposure of Basil (*Ocimum*
863 *basilicum* L.) Growing in an Organically Fertilized Peat Substrate and Strategies to Mitigate
864 Related Harmful Impacts on Plant Growth. *Front Plant Sci* 10.
865 <https://doi.org/10.3389/fpls.2019.01696>
- 866 Frostegård, Å., Vick, S.H.W., Lim, N.Y.N., Bakken, L.R., Shapleigh, J.P., 2022. Linking meta-omics to the
867 kinetics of denitrification intermediates reveals pH-dependent causes of N₂O emissions and
868 nitrite accumulation in soil. *ISME Journal* 16, 26–37. [https://doi.org/10.1038/s41396-021-](https://doi.org/10.1038/s41396-021-01045-2)
869 [01045-2](https://doi.org/10.1038/s41396-021-01045-2)
- 870 Han, Y., Zhang, M., Chen, X., Zhai, W., Tan, E., Tang, K., 2022. Transcriptomic evidences for microbial
871 carbon and nitrogen cycles in the deoxygenated seawaters of Bohai Sea. *Environ Int* 158.
872 <https://doi.org/10.1016/j.envint.2021.106889>
- 873 Hechmi, N., Aissa, N. Ben, Abdennaceur, H., Jedidi, N., 2013. Phytoremediation Potential of Maize
874 (*Zea Mays* L.) in Co-Contaminated Soils With Pentachlorophenol and Cadmium. *Int J*
875 *Phytoremediation* 15, 703–713. <https://doi.org/10.1080/15226514.2012.723067>
- 876 Jia, F., Li, Y., Hu, Q. nan, Zhang, L., Mao, L. gang, Zhu, L. zhen, Jiang, H. yun, Liu, X. gang, Sun, Y., 2023.
877 Factors impacting the behavior of phytoremediation in pesticide-contaminated environment: A
878 meta-analysis. *Science of the Total Environment* 892.
879 <https://doi.org/10.1016/j.scitotenv.2023.164418>
- 880 Kieser, S., Brown, J., Zdobnov, E.M., Trajkovski, M., McCue, L.A., 2020. ATLAS: A Snakemake workflow
881 for assembly, annotation, and genomic binning of metagenome sequence data. *BMC*
882 *Bioinformatics* 21. <https://doi.org/10.1186/s12859-020-03585-4>
- 883 Langmead, B., Salzberg, S.L., 2012. Fast gapped-read alignment with Bowtie 2. *Nat Methods* 9, 357—
884 359. <https://doi.org/10.1038/nmeth.1923>
- 885 Liang, C., Amelung, W., Lehmann, J., Kästner, M., 2019. Quantitative assessment of microbial
886 necromass contribution to soil organic matter. *Glob Chang Biol* 25, 3578–3590.
887 <https://doi.org/10.1111/gcb.14781>
- 888 Lin, Q., Shen, K.L., Zhao, H.M., Li, W.H., 2008. Growth response of *Zea mays* L. in pyrene-copper co-
889 contaminated soil and the fate of pollutants. *J Hazard Mater* 150, 515–521.
890 <https://doi.org/10.1016/j.jhazmat.2007.04.132>
- 891 Liu, S., Liu, H., Chen, R., Ma, Y., Yang, B., Chen, Z., Liang, Y., Fang, J., Xiao, Y., 2021. Role of two plant
892 growth-promoting bacteria in remediating cadmium-contaminated soil combined with
893 *miscanthus floridulus* (Lab.). *Plants* 10. <https://doi.org/10.3390/plants10050912>
- 894 Liu, X., Selonen, V., Steffen, K., Surakka, M., Rantalainen, A.L., Romantschuk, M., Sinkkonen, A., 2019.
895 Meat and bone meal as a novel biostimulation agent in hydrocarbon contaminated soils.
896 *Chemosphere* 225, 574–578. <https://doi.org/10.1016/j.chemosphere.2019.03.053>
- 897 Li, Yijia, Ma, J., Li, Yuqian, Xiao, C., Shen, X., Chen, J., Xia, X., 2022. Nitrogen addition facilitates
898 phytoremediation of PAH-Cd cocontaminated dumpsite soil by altering alfalfa growth and

- 899 rhizosphere communities. *Science of the Total Environment* 806.
900 <https://doi.org/10.1016/j.scitotenv.2021.150610>
- 901 Mallick, H., Rahnavard, A., McIver, L.J., Ma, S., Zhang, Y., Nguyen, L.H., Tickle, T.L., Weingart, G., Ren,
902 B., Schwager, E.H., Chatterjee, S., Thompson, K.N., Wilkinson, J.E., Subramanian, A., Lu, Y.,
903 Waldron, L., Paulson, J.N., Franzosa, E.A., Bravo, H.C., Huttenhower, C., 2021. Multivariable
904 association discovery in population-scale meta-omics studies. *PLoS Comput Biol* 17.
905 <https://doi.org/10.1371/journal.pcbi.1009442>
- 906 Mondini, C., Cayuela, M.L., Sinicco, T., Sánchez-Monedero, M.A., Bertolone, E., Bardi, L., 2008. Soil
907 application of meat and bone meal. Short-term effects on mineralization dynamics and soil
908 biochemical and microbiological properties. *Soil Biol Biochem* 40, 462–474.
909 <https://doi.org/10.1016/J.SOILBIO.2007.09.010>
- 910 Naskar, S., Hohl, M., Tassinari, M., Low, H.H., 2021. The structure and mechanism of the bacterial
911 type II secretion system. *Mol Microbiol*. <https://doi.org/10.1111/mmi.14664>
- 912 Nigris, S., Baldan, E., Tondello, A., Zanella, F., Vitulo, N., Favaro, G., Guidolin, V., Bordin, N., Telatin,
913 A., Barizza, E., Marcato, S., Zottini, M., Squartini, A., Valle, G., Baldan, B., 2018. Biocontrol traits
914 of *Bacillus licheniformis* GL174, a culturable endophyte of *Vitis vinifera* cv. Glera. *BMC Microbiol*
915 18, 1–16. <https://doi.org/10.1186/s12866-018-1306-5>
- 916 Nwosu, O.U., Nwoko, C.O., Agu, C.M., Njoku, P.C., Chigbo, C.O., 2018. Assessment of remediation
917 Potentials of maize (*Zea mays*) on sites co-contaminated with Pb and anthracene. *International*
918 *Journal of Advanced Engineering, Management and Science* 4, 664–670.
919 <https://doi.org/10.22161/ijaems.4.9.4>
- 920 Pacwa-Płociniczak, M., Czapla, J., Płociniczak, T., Piotrowska-Seget, Z., 2019. The effect of
921 bioaugmentation of petroleum-contaminated soil with *Rhodococcus erythropolis* strains on
922 removal of petroleum from soil. *Ecotoxicol Environ Saf* 169, 615–622.
923 <https://doi.org/10.1016/j.ecoenv.2018.11.081>
- 924 Pacwa-Płociniczak, M., Płaza, G.A., Piotrowska-Seget, Z., 2016. Monitoring the changes in a bacterial
925 community in petroleum-polluted soil bioaugmented with hydrocarbon-degrading strains.
926 *Applied Soil Ecology* 105, 76–85. <https://doi.org/10.1016/j.apsoil.2016.04.005>
- 927 Pena, R.T., Blasco, L., Ambroa, A., González-Pedrajo, B., Fernández-García, L., López, M., Bleriot, I.,
928 Bou, G., García-Contreras, R., Wood, T.K., Tomás, M., 2019. Relationship between quorum
929 sensing and secretion systems. *Front Microbiol*. <https://doi.org/10.3389/fmicb.2019.01100>
- 930 Phillips, L.A., Germida, J.J., Farrell, R.E., Greer, C.W., 2008. Hydrocarbon degradation potential and
931 activity of endophytic bacteria associated with prairie plants. *Soil Biol Biochem* 40, 3054–3064.
932 <https://doi.org/10.1016/J.SOILBIO.2008.09.006>
- 933 Płociniczak, T., Fic, E., Pacwa-Płociniczak, M., Pawlik, M., Piotrowska-Seget, Z., 2017. Improvement of
934 phytoremediation of an aged petroleum hydrocarbon-contaminated soil by *Rhodococcus*
935 *erythropolis* CD 106 strain. *Int J Phytoremediation* 19.
936 <https://doi.org/10.1080/15226514.2016.1278420>
- 937 Powell, S.M., Ferguson, S.H., Bowman, J.P., Snape, I., 2006. Using real-time PCR to assess changes in
938 the hydrocarbon-degrading microbial community in Antarctic soil during bioremediation.
939 *Microb Ecol* 52, 523–532. <https://doi.org/10.1007/s00248-006-9131-z>

- 940 Prieto, P., Mercado-Blanco, J., 2008. Endophytic colonization of olive roots by the biocontrol strain
941 *Pseudomonas fluorescens* PICF7. <https://doi.org/10.1111/j.1574-6941.2008.00450.x>
- 942 Qi, X., Wu, W., Shah, F., Peng, S., Huang, J., Cui, K., Liu, H., Nie, L., 2012. Ammonia volatilization from
943 urea-application influenced germination and early seedling growth of dry direct-seeded rice.
944 *The Scientific World Journal* 2012. <https://doi.org/10.1100/2012/857472>
- 945 Sánchez-Castro, I., Molina, L., Prieto-Fernández, M.Á., Segura, A., 2023. Past, present and future
946 trends in the remediation of heavy-metal contaminated soil - Remediation techniques applied
947 in real soil-contamination events. *Heliyon*. <https://doi.org/10.1016/j.heliyon.2023.e16692>
- 948 Sánchez-Monedero, M.A., Mondini, C., Cayuela, M.L., Roig, A., Contin, M., De Nobili, M., 2008.
949 Fluorescein diacetate hydrolysis, respiration and microbial biomass in freshly amended soils.
950 *Biol Fertil Soils* 44, 885–890. <https://doi.org/10.1007/s00374-007-0263-1>
- 951 Sei, K., Asano, K.I., Tateishi, N., Mori, K., Ike, M., Fujita, M., 1999. Design of PCR primers and gene
952 probes for the general detection of bacterial populations capable of degrading aromatic
953 compounds via catechol cleavage pathways. *J Biosci Bioeng* 88, 542–550.
954 [https://doi.org/10.1016/S1389-1723\(00\)87673-2](https://doi.org/10.1016/S1389-1723(00)87673-2)
- 955 Shtangeeva, I., Luiho, J.V.P., Kahelin, H., Gobran, G.R., 2004. Improvement of phytoremediation
956 effects with help of different fertilizer. *Soil Sci Plant Nutr* 50, 885–889.
957 <https://doi.org/10.1080/00380768.2004.10408550>
- 958 Sułowicz, S., Cycoń, M., Piotrowska-Seget, Z., 2016. Non-target impact of fungicide tetraconazole on
959 microbial communities in soils with different agricultural management. *Ecotoxicology* 25, 1047–
960 1060. <https://doi.org/10.1007/s10646-016-1661-7>
- 961 Sun, Y., Rantalainen, A.L., Romantschuk, M., Sinkkonen, A., 2018. Requirement of ecological
962 replication with independent parallel analysis of each replicate plot to support soil remediation.
963 *Int Biodeterior Biodegradation* 133, 133–141. <https://doi.org/10.1016/J.IBIOD.2018.06.006>
- 964 Su, X., Xue, B., Wang, Y., Za, M., Lin, H., Chen, J., Mei, R., Wang, Z., Sun, F., 2019. Ecotoxicology and
965 Environmental Safety Bacterial community shifts evaluation in the sediments of Puyang River
966 and its nitrogen removal capabilities exploration by resuscitation promoting factor 179, 188–
967 197. <https://doi.org/10.1016/j.ecoenv.2019.04.067>
- 968 Ullah, S., Liu, Q., Wang, S., Jan, A.U., Sharif, H.M.A., Ditta, A., Wang, G., Cheng, H., 2023. Sources,
969 impacts, factors affecting Cr uptake in plants, and mechanisms behind phytoremediation of Cr-
970 contaminated soils. *Science of the Total Environment*.
971 <https://doi.org/10.1016/j.scitotenv.2023.165726>
- 972 Wu, T., Hu, E., Xu, S., Chen, M., Guo, P., Dai, Z., Feng, T., Zhou, L., Tang, W., Zhan, L., Fu, X., Liu, S., Bo,
973 X., Yu, G., 2021. clusterProfiler 4.0: A universal enrichment tool for interpreting omics data.
974 *Innovation* 2. <https://doi.org/10.1016/j.xinn.2021.100141>
- 975 Yousaf, S., Ripka, K., Reichenauer, T.G., Andria, V., Afzal, M., Sessitsch, A., 2010. Hydrocarbon
976 degradation and plant colonization by selected bacterial strains isolated from Italian ryegrass
977 and birdsfoot trefoil. *J Appl Microbiol* 109, 1389–1401. <https://doi.org/10.1111/j.1365-2672.2010.04768.x>

979 Zhang, H., Dang, Z., Zheng, L.C., Yi, X.Y., 2009. Remediation of soil co-contaminated with pyrene and
980 cadmium by growing maize (*Zea mays* L.). *International Journal of Environmental Science and*
981 *Technology* 6, 249–258. <https://doi.org/10.1007/BF03327629>

982

983

984

985

986

987

988

989

990

991

992

993

994

995

996

997

998

999

1000

1001

1002

1003

1004

1005

1006 Supplementary materials

1007

1008 *The potential of enhanced phytoremediation to clean up multi-contaminated soil – insights from*

1009 *metatranscriptomics*

1010

1011 Magdalena Pacwa-Płociniczak^{1*}, Agata Kumor¹, Marta Bukowczan¹, Aki Sinkkonen², Marja

1012 Roslund², Tomasz Płociniczak^{1*}

1013

1014 ¹Institute of Biology, Biotechnology and Environmental Protection, Faculty of Natural

1015 Sciences, University of Silesia in Katowice, Jagiellońska 28, 40-032 Katowice, Poland

1016 ² Horticulture Technologies, Natural Resources Institute Finland, Itäinen Pitkätatu 4A, Turku,

1017 Finland

1018

1019 * - corresponding authors: magdalena.pacwa-plociniczak@us.edu.pl;

1020 tomasz.plociniczak@us.edu.pl; tel +48322009442

1021

1022

1023

1024

1025

1026

1027

1028

1029

1030

1031 Table S1. Selected physicochemical properties of the soil used in the experiment.

Parameter	Soil	Soil+MBM
Sand [%]	80.37 ± 0.06	79.88 ± 0.17
Silt [%]	17.83 ± 0.06	17.95 ± 0.03
Clay [%]	1.8 ± 0.00	2.17 ± 0.15
Textural classification	Loamy sand	Loamy sand
Organic matter [%]	4.03 ± 0.15	17.03 ± 0.47
pH _{H2O}	6.97 ± 0.15	6.33 ± 0.21
N total [% N]	0.63 ± 0.10	2.47 ± 0.40
Fe [mg kg ⁻¹]	11402 ± 509	9701 ± 214
P total [%]	0.039 ± 0.003	1.01 ± 0.08
C organic [%]	2.62 ± 0.19	6.88 ± 0.42

1032 ± Stand. Dev. of three independent experiments; ; MBM – meat and bone meal.

1033

1034

1035

1036

1037

1038

1039

1040

1041

1042

1043

1044

1045

1046

1047

1048

1049

1050

1051 Table S2. Primers used for PCR amplification.

Primer	Sequence (5'-3')	Gene	Annealing (°C)	Reference
pvdF-F	TACATCCTCGATGCCGACCT	<i>pvd</i>	57	MBG8561616.1*
pvdF-R	CAGGTCGATCATGGTAGCCC			
dcyD-F	CTCGAACGCTTCAAACGCC	<i>dcyD</i>	57	MBG8561384.1*
dcyD-R	GCTTGATGTAGATGTGCGCGC			
bfr-F	TGCACAAGGACTACGTCAGC	<i>bfr</i>	57	MBG8560256.1*
bfr-R	TTGATCAGACCCTGCTGCTT			
tonB-F	CTACGAGTTCGGCTACAGCG	<i>tonB</i>	57	MBG8561215.1*
tonB-R	CACGGTGACCTTCTGGATGG			
cysA-F	TCAAGAACACCCAGGGCAAG	<i>cysA</i>	57	MBG8561413.1*
cysA-R	TCAAGAACACCCAGGGCAAG			
pstA-F	CGCGAAGTCGAGATCAACCT	<i>pstA</i>	57	MBG8558409.1*
pstA-R	CCCACACCTTGGCGAAGTAG			
gcd-F	AGATCACCCCGAACAACGTG	<i>gcd</i>	57	MBG8562075.1*
gcd-R	TTCTCGTTGGTCAGCTCGAC			
pqqA-F	CGTCTTCTACTGTCGCTCCG	<i>pqqA</i>	57	MBG8558041.1*
pqqA-R	CAGGCCATCACGGTACCAG			
acdS-F	GATTTGCCCTCGTAGACCGG	<i>acdS</i>	57	MBG8559878.1*
acdS-R	ATCCGGAATATGGCTTGCCC			
entD-F	CGCTGACCTTCTCCCTCAAG	<i>entD</i>	57	MBG8562760.1*
entD-R	GCGGACCATTCCAGCAGTTC			
pE	AAACTCAAAGGAATTGACGG	16S rRNA	57	(Edwards et al.,
pF•	ACGAGCTGACGACAGCCATG			1989)
alkB-F	AACTACMTCGARCAYTACGG	<i>alkB</i>	57	(Powell et al.,
alkB-R	TGAMGATGTGGTYRCTGTTC			2006)
alk-H1-F	CIGIICACGAIITIGGICACAAGAAGG	<i>alkH</i>	55	(Phillips et al.,
alk-H3-R	IGCITGITGATCIIIIGTGICGCTGIAG			2008)

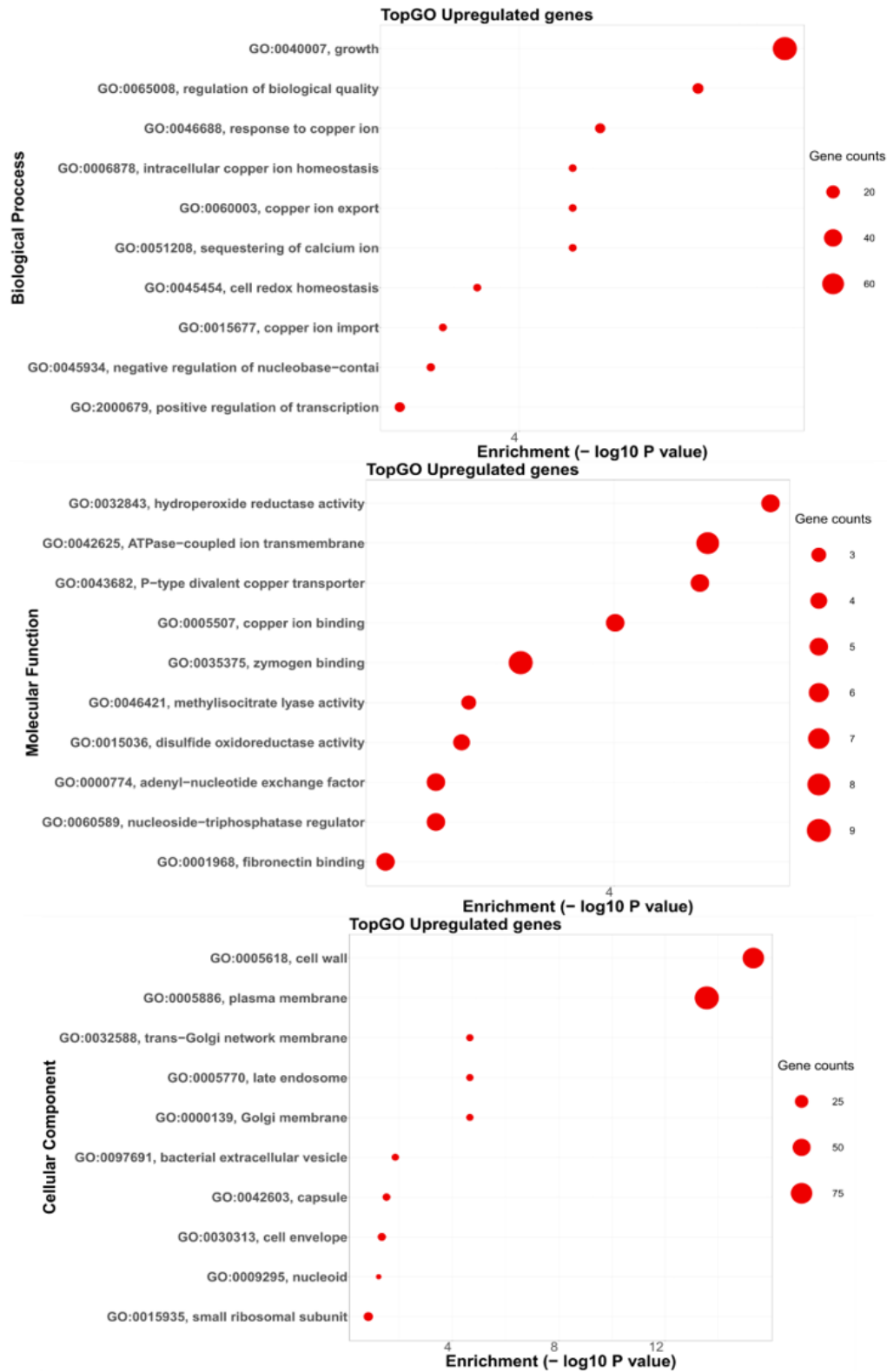
ladA-F	GCAGTTCGTGAAGCTGTTCA	<i>ladA</i>	57	MBG8560652.1*
ladA-R	GAGAAGGTGACAGCGAATGC			
P450fw1	GTSGGCGGCAACGACACSAC	CYP153	58	(Yousaf et al.,
P450rv3	GCASCGGTGGATGCCGAAGCCRA			2010)
C120F	GCCAACGTCGACGTCTGGCAGCA	C120	59	(Sei et al., 1999)
C120R	CGCCTTCAAAGTTGATCTGCGTGGTTGGT			
C230F	AAGAGGCATGGGGGCGCACCGGTTCGA	C230	57	(Sei et al., 1999)
C230R	TCACCAGCAAACACCTCGTTGCGGTTGCC			

1052 * accession numbers from GenBank

1053

1054

1055



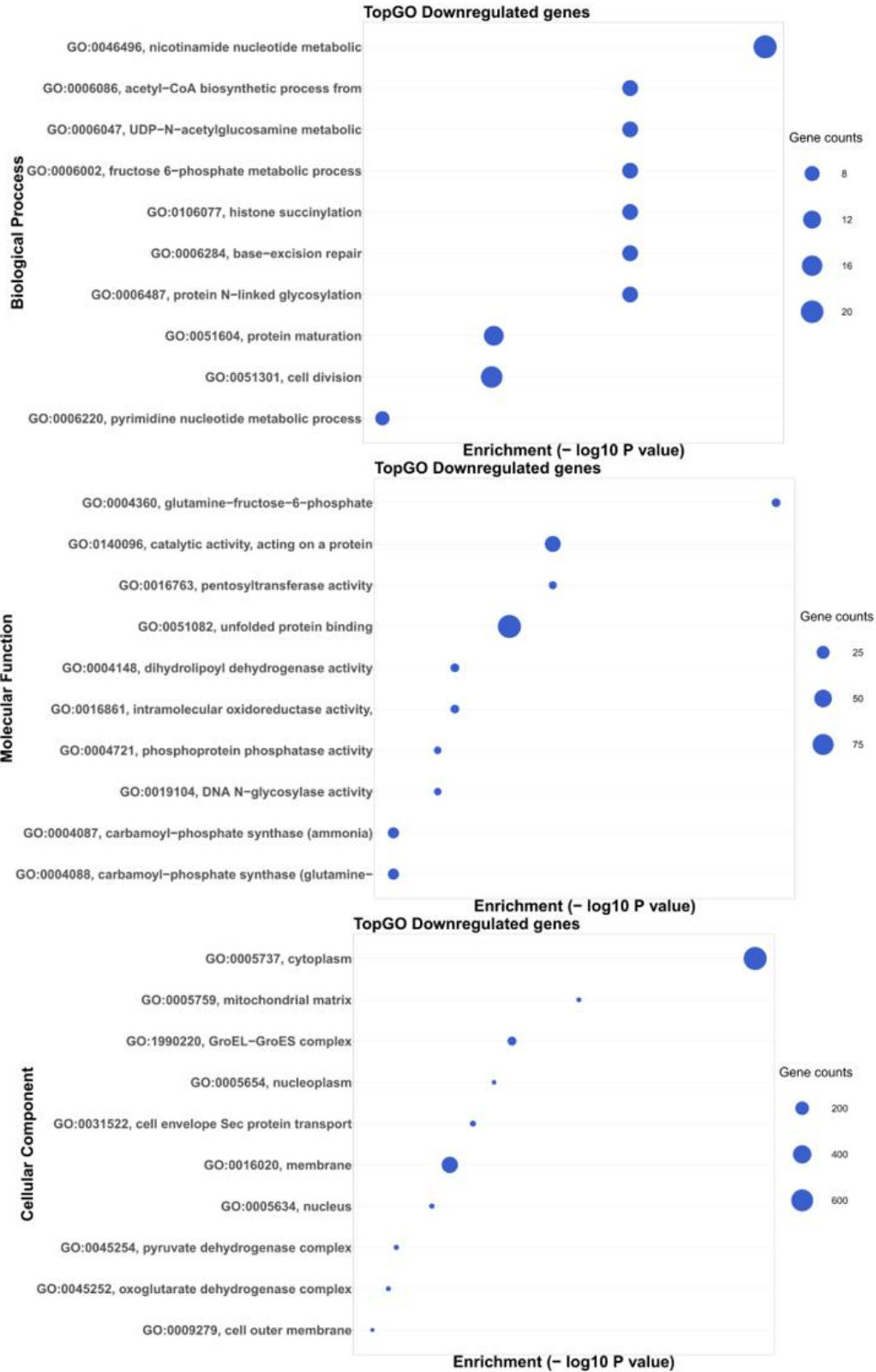
1056

1057 Fig. S1 GO enrichment analysis of up-regulated genes in response to BL+MBM treatment;

1058 BL – live bacteria; MBM – meat and bone meal.

1059

1060

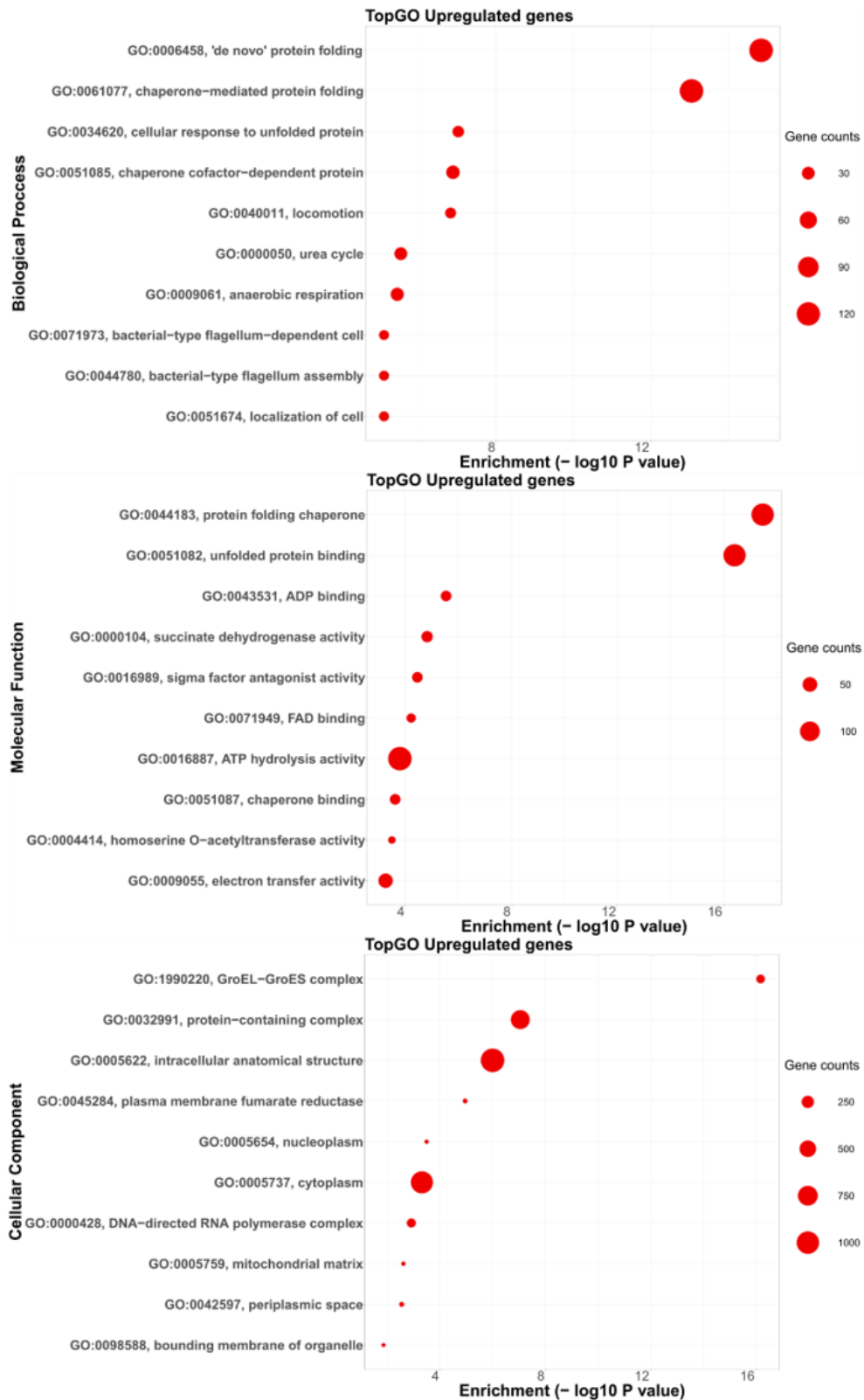


1061

1062 Fig. S2 GO enrichment analysis of down-regulated genes in response to BL+MBM treatment;

1063 BL – live bacteria; MBM – meat and bone meal.

1064

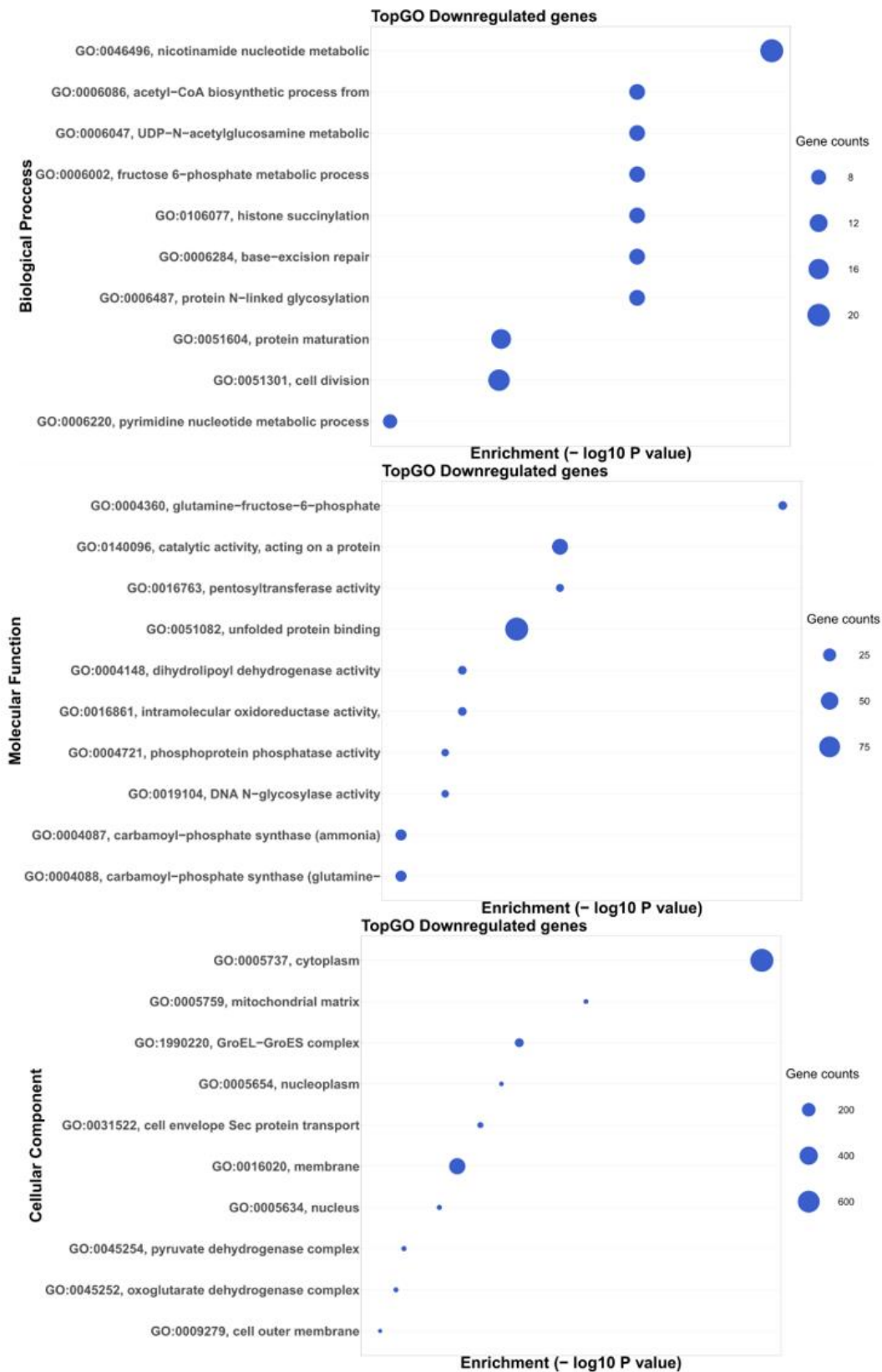


1065

1066 Fig. S3 GO enrichment analysis of up-regulated genes in response to W+MBM treatment; W –

1067 water; MBM – meat and bone meal.

1068



1069

1070 Fig. S4 GO enrichment analysis of down-regulated genes in response to W+MBM treatment;

1071 W – water; MBM – meat and bone meal.